JCTC Journal of Chemical Theory and Computation

pubs.acs.org/JCTC Article

Seniority and Hierarchy Configuration Interaction for Radicals and Excited States

Fábris Kossoski* and Pierre-François Loos*

Cite This: J. Chem. Theory Comput. 2023, 19, 8654−8670 Read Online

ACCESS | Metrics & More | Article Recommendations | Supporting Information

ABSTRACT: Hierarchy configuration interaction (hCI) has recently been introduced as an alternative configuration interaction (CI) route combining excitation degree and seniority number and has been shown to efficiently recover both dynamic and static correlations for closed-shell molecular systems [*J. Phys. Chem. Lett.* **2022**, *13*, 4342]. Here we generalize hCI for an arbitrary reference determinant, allowing calculations for radicals and excited states in a state-specific way. We gauge this route against excitation-based CI (eCI) and seniority-based CI (sCI) by evaluating how different ground-state properties of radicals converge to the full CI limit. We find that hCI outperforms or matches eCI, whereas sCI is far less accurate, in line with previous observations for closed-shell molecules. Employing second-order Epstein−Nesbet (EN2) perturbation theory as a correction significantly accelerates the convergence of hCI and eCI. We further explore various hCI and sCI models to calculate the excitation energies of closed- and open-shell systems. Our results underline that the choice of both the reference determinant and the set of orbitals drives the fine balance between correlation of ground and excited states. State-specific hCI2 and higher-order models perform similarly to their eCI counterparts, whereas lower orders of hCI deliver poor results unless supplemented by the EN2 correction, which substantially improves their accuracy. In turn, sCI1 produces decent excitation energies for radicals, encouraging the development of related seniority-based coupled-cluster methods.

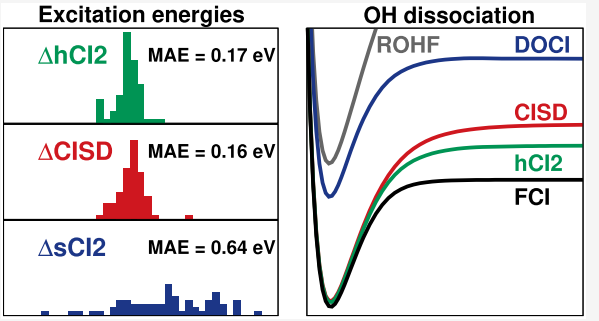

I. INTRODUCTION

Configuration interaction (CI) offers a systematic way to solve the many-body electronic structure problem.[1,2] By including progressively more determinants in the Hilbert space, the wave function becomes increasingly closer to the exact one, and so does the electronic energy. In full CI (FCI), all determinants are accounted for, and the problem is solved exactly (for a given basis set). In practice, however, one resorts to approximate CI models where only the determinants that satisfy a given criterion are included in the truncated Hilbert space.

The most well-known CI route is based on the excitation degree *e*. Starting from a reference determinant, typically the Hartree−Fock (HF) determinant, one generates all connected determinants by exciting at most *e* electrons. The excitation degree thus defines the order of the approximate excitation-based CI (eCI) model: CI with single excitations (CIS), CI with single and double excitations (CISD), CI with single, double, and triple excitations (CISDT), etc. The eCI route rather quickly captures dynamic (weak) correlation, though it struggles with the description of static (strong) correlation.

A different CI route is based on the seniority number *s* (the number of unpaired electrons in a given determinant). In seniority-based CI (sCI),[3−6] there is no reference determinant, and one accounts for all determinants having seniority equal to or less than *s*. In contrast to eCI, sCI recovers static correlation more efficiently and works well to describe molecular dissociation[7−9] at the expense of a poorer account of dynamic correlation and a higher computational cost. For systems with an even number of electrons, the first approximate model is defined by $s = 0$ (sCI0), usually referred to as doubly occupied CI (DOCI), which is followed by the higher-order models sCI2, sCI4, and so on. For odd numbers of electrons, the seniority route follows along odd numbers of *s*: sCI1, sCI3, and so on.

We have recently introduced a third CI route, hierarchy CI (hCI),[10] where the Hilbert space is partitioned according to a hierarchy parameter *h* that combines the excitation degree *e* and the seniority number *s*, defined as $h = (e + s/2)/2$. This definition ensures that all classes of determinants whose numbers share the same scaling with system size are included at the same hierarchy *h*. This key feature distinguishes hCI from previous schemes combining excitation and seniority.[8,11,12] By allowing for higher-order excitations of paired electrons (as explained in detail below), hCI is reminiscent of perfect pairing models for closed-shell systems.[13−19] For different properties

Received: August 28, 2023
Revised: October 25, 2023
Accepted: October 27, 2023
Published: November 15, 2023

https://doi.org/10.1021/acs.jctc.3c00946
J. Chem. Theory Comput. 2023, 19, 8654−8670

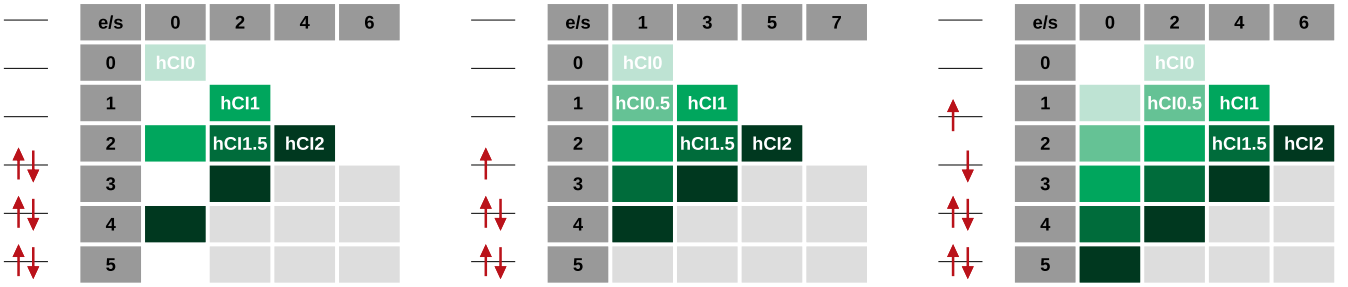

Figure 1. Partitioning of the Hilbert space according to the seniority number s and the excitation degree e with respect to a given reference determinant (shown by its side) for a closed-shell reference (left), an open-shell reference with one unpaired electron (center), and an open-shell reference with two unpaired electrons (right). The color tones represent the determinants that are included at a given hCI model. hCI0 reduces to the reference determinant (usually the HF solution) in the former two cases, where $s_0 = 0$ and $s_0 = 1$.

and closed-shell molecular systems, hCI was found to display an overall faster convergence toward the FCI results than the traditional eCI route.[10] In this sense, it was able to recover both static and dynamic correlations more effectively than either eCI or sCI. However, hCI has been defined only for a closed-shell reference, thus being limited to the ground state of systems with an even number of electrons.

There are two possible approaches to target excited states with the CI methods. One can employ the ground-state HF orbitals and obtain excitation energies from the higher-lying eigenvalues of the CI matrix, which we refer to as the ground-state-based approach. Instead, one may optimize the orbitals for the excited state of interest (described with an appropriate reference), followed by a separate CI calculation, in a so-called state-specific approach (ΔCI). There has been a recent surge in the development of state-specific methods, covering single-reference and multiconfigurational self-consistent field,[20−31] density functional theory,[32−44] perturbation theory,[45−47] quantum Monte Carlo,[48−56] and coupled-cluster (CC)[57−63] methods. In particular, by employing a minimal configuration state function (CSF) reference, we have recently shown that excitation-based ΔCI models deliver far more accurate excitation energies than their ground-state-based analogs.[29]

Here, our first goal is to generalize hCI for an arbitrary type of reference, thus extending its applicability from ground-state closed-shell[10] to radical and state-specific excited-state calculations. This is shown in section II. The computational details of the implementation and the specific calculations performed here are presented in section III. In section IV A, we assess the performance of hCI, eCI, and sCI models by calculating various properties of four ground-state radicals, which comprises our second goal. Our third goal is to evaluate how perturbation theory, more precisely the second-order Epstein−Nesbet (EN2) perturbative correction (both standard and renormalized),[64] impacts various properties of ground-state closed-shell systems and radicals for hCI, eCI, and sCI models. This part is presented in section IV B. Inspired by the results of hCI for ground-state closed-shell systems[10] and by the promising set of excitation-based ΔCI methods,[29] here we explore hCI models for excited states, following both the ground-state-based and state-specific approaches. In this sense, our fourth goal is to assess the accuracy of hCI models for excited states, which is the subject of section IV C. Furthermore, to the best of our knowledge, sCI models have not yet been directly used to target excited states, despite the growing number of methods that exploit the concept of seniority for both ground[61,65−81] and excited states.[60−62,79,81−86] Our fifth goal, detailed in section IV D, is therefore to define and gauge ground-state-based and state-specific sCI models for excited states. Finally, in section IV E we assess how the excitation energies are impacted by the EN2 perturbative correction to hCI and sCI models, our sixth and last goal. Section V closes the present contribution with the main conclusions and perspectives.

II. HIERARCHY CONFIGURATION INTERACTION

We introduced hCI[10] as a particular truncation of the Hilbert space, viewed as a two-dimensional map of determinants built from their seniority s and their excitation degree e with respect to a reference determinant, as shown in Figure 1. By defining orbital subspaces according to the occupancy in the reference determinant (doubly occupied, singly occupied, or unoccupied), we refer to the class of an excited determinant as the combination of the number of electrons and seniority in each orbital subspace. The number of determinants N_{det} within a given class scales polynomially with the number of basis functions N, with the exponent depending on the specific class. For instance, for the class of doubly excited determinants with no unpaired electrons ($e = 2$ and $s = 0$), $N_{det} = O(N^2)$. hCI was defined such that, at a given hierarchy h, all classes of determinants presenting a scaling of $N_{det} = O(N^{2h})$ or less are accounted for. This means moving diagonally in the seniority−excitation map (denoted by the color tones in Figure 1). In comparison, eCI spans the map horizontally (top to bottom), whereas sCI does it vertically (left to right).

hCI was initially introduced for a closed-shell reference (left panel of Figure 1).[10] Here we generalize it for an arbitrary Slater determinant reference, including systems with an odd number of electrons. With respect to a given reference determinant, we define the hierarchy h of a candidate determinant to be included in the truncated hCI model as

$$h = \frac{e + (s - s_0)/2}{2} \tag{1}$$

where s and s_0 denote the seniorities of the candidate and reference determinants, respectively, and e represents the excitation degree that connects them. The definition in eq 1 guarantees the sought-after relation between the classes of determinants and their scaling. Namely, all classes whose number of determinants N_{det} share the same scaling with N enter at the hierarchy h. Had we employed the absolute value of $s - s_0$ or discarded s_0 in the definition of h, this property would not hold. The term $(s - s_0)/2$ is always an integer, with s and s_0 being even (odd) for systems with even (odd) numbers of electrons.

https://doi.org/10.1021/acs.jctc.3c00946
J. Chem. Theory Comput. 2023, 19, 8654−8670

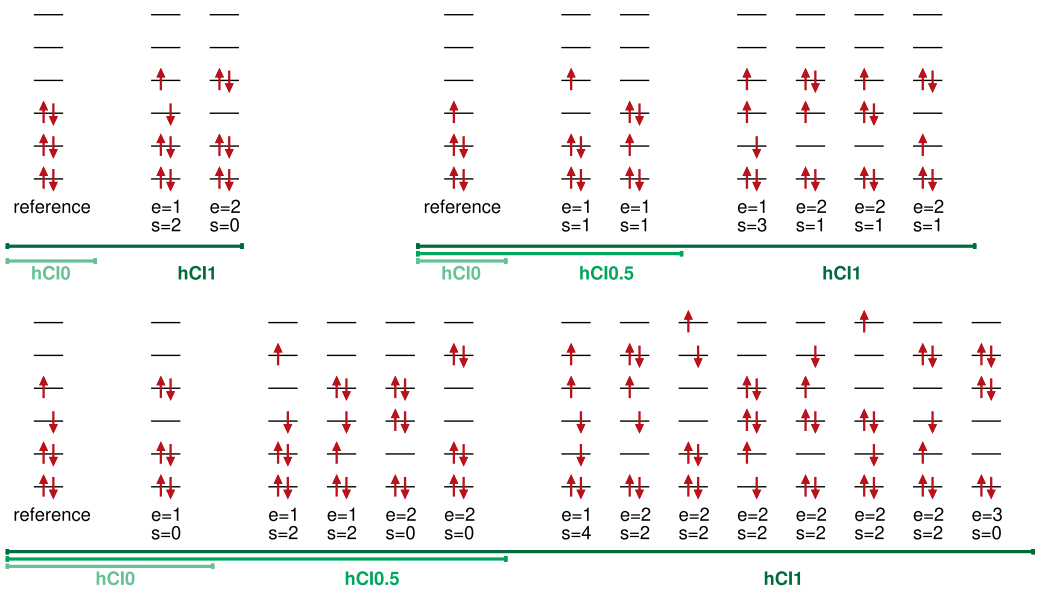

Figure 2. Classes of determinants generated in hCI0, hCI0.5, and hCI1 for three different reference determinants: closed-shell (top left), open-shell with one unpaired electron (top right), and open-shell with two unpaired electrons (bottom). By dividing the orbitals of the reference determinant into doubly occupied, singly occupied, and unoccupied subspaces, the class of an excited determinant is defined by the number of electrons and seniority in each orbital subspace.

The excitation degree e is also an integer. Therefore, h assumes integer or half-integer values for any type of reference determinant. For a given hCI model defined by h, we include all of the candidate determinants having a hierarchy less than or equal to h with respect to any determinant in the reference. This definition allows us to build multireference hCI models as well. Notice that eq 1 simplifies to the previous definition[10] for the case of a closed-shell reference determinant, where $s_0 = 0$. hCI can be viewed as a CI model that includes increasingly more dissimilar determinants with respect to a given reference determinant. The level of dissimilarity is represented by the hierarchy h, which accounts for differences in orbital occupation (through the excitation degree e) and differences in the number of unpaired electrons [through the term $(s - s_0)/2$].

We show in Figure 1 how the seniority−excitation map of determinants is partitioned for a closed-shell reference ($s_0 = 0$) and for open-shell references with one ($s_0 = 1$) or two ($s_0 = 2$) unpaired electrons. For these three types of references, the classes of determinants including up to hCI1 are presented in Figure 2. The closed-shell reference determinant is the natural choice for describing the ground state of a closed-shell system as well as its doubly excited states.[29,36,37,59−61] Meanwhile, a determinant having one unpaired electron is suitable for an open-shell system with doublet ground and excited states. Singlet and triplet singly excited states of closed-shell systems as well as diradicals[87−89] would require a reference determinant with two unpaired electrons.

In eCI, the number of determinants N_{det} scales polynomially with the number of basis functions N as N^{2e}.[1] Likewise, in hCI, N_{det} scales as N^{2h}. The actual computational cost scales as $O(N^{2e+2})$ for eCI and similarly for hCI, scaling as $O(N^{2h+2})$. Both the scaling of N_{det} and the computational scaling along the two routes are shown in Table I. As for sCI models, the scaling of N_{det} with respect to N is exponential at all orders.[3−6] This is the case because excitations of all degrees are included, even at lower orders such as sCI0 and sCI1.

Table I. Scaling of N_{det} and Computational Scaling (Cost) in Terms of the Number of Basis Functions N for the Hierarchy- and Excitation-Based CI Routes, with and without the EN2 Perturbative Correction

hierarchy-based		excitation-based		N_{det}	cost
hCI1		CIS		$O(N^2)$	$O(N^4)$
hCI1.5				$O(N^3)$	$O(N^5)$
hCI2	hCI1+EN2	CISD	CIS+EN2	$O(N^4)$	$O(N^6)$
hCI2.5	hCI1.5+EN2			$O(N^5)$	$O(N^7)$
hCI3	hCI2+EN2	CISDT	CISD+EN2	$O(N^6)$	$O(N^8)$
hCI3.5	hCI2.5+EN2			$O(N^7)$	$O(N^9)$
hCI4	hCI3+EN2	CISDTQ	CISDT +EN2	$O(N^8)$	$O(N^{10})$

For a closed-shell reference determinant ($s_0 = 0$), hCI0 reduces to the reference determinant, usually chosen as the HF one. The first nontrivial order is hCI1 (see the left panel of Figure 1), which accounts for all single excitations (as CIS) plus all paired double excitations (two electrons promoted from the same occupied orbital into the same virtual orbital), as shown in the top left panel of Figure 2. For both classes of determinants, their numbers scale as N^2 and are thus taken into account at the same hierarchy of hCI ($h = 1$ in this case). An odd number of excitations from a closed-shell reference always leaves unpaired electrons, hence the empty blocks at $s = 0$ for odd e. hCI1.5 augments the set of hCI1 determinants with the set of double excitations where two electrons are unpaired. At the next integer order, hCI2 incorporates all classes of determinants where N_{det} scales as N^4. In total, it accounts for all single and double excitations (as CISD) plus the subset of triple excitations that leave only two unpaired electrons plus the subset of quadruple excitations where no electrons are unpaired.

For an odd number of electrons, s assumes odd values starting from $s = 1$. The simplest reference is an open-shell determinant with one unpaired electron ($s_0 = 1$), shown in the center panel of Figure 1 and in the top right panel of Figure 2. hCI0 also reduces

https://doi.org/10.1021/acs.jctc.3c00946
J. Chem. Theory Comput. 2023, 19, 8654−8670

to the reference determinant (the restricted open-shell HF solution is a natural choice). In contrast to the closed-shell case, here there are no empty blocks in the seniority−excitation map. Actually, the hCI series displays the hCI0.5 level, accounting only for the single excitations from and into the singly occupied orbital. When HF orbitals are employed, these excitations do not connect with the reference, and in this case, hCI0.5 provides the same energy as restricted open-shell HF. More generally, since there are more types of orbitals for the open-shell reference (doubly occupied, singly occupied, and unoccupied) than for the closed-shell reference (doubly occupied or unoccupied), there are correspondingly more classes of determinants at a given level of hCI. This can be appreciated from the comparison of hCI1 for closed- and open-shell references, shown in Figure 2.

Finally, one can employ a reference determinant having more unpaired electrons to define hCI models. The case of two unpaired electrons ($s_0 = 2$) is shown in the right panel of Figure 1. The key difference in the hCI sequence with respect to the closed-shell case lies in the displacement by one block to the right in the seniority−excitation map, reflecting the shift from the seniority-zero reference to the seniority-two reference. In addition, in the two previous cases, the hCI0 level only included the reference determinant whereas for $s_0 = 2$, hCI0 accounts not only for the reference determinant but also for the two closed-shell determinants produced by the single excitation that pairs the two unpaired electrons. The hCI1 classes of determinants for the $s_0 = 2$ reference can be seen in the bottom of Figure 2, which clearly outnumber the fewer classes associated with the $s_0 = 0$ and $s_0 = 1$ cases.

One could adopt references with even larger s_0, further displacing the hCI sequence to the right in the seniority−excitation map. In this case, hCI0 would include all of the lower-spin determinants obtained by partially or totally pairing the unpaired electrons. Notice that the number of such determinants does not depend on the system size (scaling as N^0) and are thus included at the $h = 0$ level, in line with the spirit of hCI. In a similar fashion, hCI can be built on top of a larger s_0 reference for odd numbers of electrons. The deductions for the number of determinants in a given hCI model for the $s_0 = 0$ closed-shell, $s_0 = 1$ open-shell, and arbitrary reference determinant can be found in Appendix A.

For a reference containing unpaired electrons, an approximate CI model generally produces spin-contaminated states. One can impose the solutions to have a well-defined spin by including additional determinants generated via higher-order hierarchies, which account for the missing spin-flip configurations.[90] The spin-contamination problem and its solution are therefore equivalent to that encountered in eCI.[91] Here we employed this procedure and considered pure spin states. For the calculation of excitation energies, however, we have also assessed the effect of not imposing this condition.

For the $s_0 = 2$ reference, one could alternatively employ a high-spin triplet determinant (two unpaired spin-up electrons) rather than the low-spin determinant shown in Figure 1. Regardless of the choice, hCI (like eCI) produces the same energies for the triplet states provided that a spin eigenstate is imposed.

III. COMPUTATIONAL DETAILS

The hCI models introduced here were implemented in QUANTUM PACKAGE[64] through a straightforward modification of the configuration interaction using a perturbative selection made iteratively (CIPSI) algorithm.[92−95] By allowing only for the determinants that are connected with the reference determinant(s) up to a given maximum hierarchy h, the CIPSI algorithm is restricted to the truncated Hilbert space specified by the reference determinant(s) and the value of h. QUANTUM PACKAGE[64] was also employed to perform all the present eCI, sCI, and FCI calculations. In a given calculation, the energies are considered to be converged when the (largest) EN2 correction computed in the truncated Hilbert space lies below 0.01 mE_h.[96] This selected CI procedure requires considerably fewer determinants than the total number of determinants in the truncated Hilbert space while delivering fairly converged energies. The ground- and excited-state CI energies are obtained with the Davidson iterative algorithm.[97]

For a given approximate CI model, we further evaluated the standard and renormalized EN2 perturbative corrections.[64] This calculation involves a single loop over the determinants left outside the truncated (internal) space but connected to it via, at most, double excitations. Looping over these external doubly excited determinants has a computational scaling equal to N_{det}, thus $O(N^{2e+4})$ for eCI and $O(N^{2h+4})$ for hCI, where e or h defines the internal CI space. For example, hCI2 and CISD present an $O(N^6)$ computational scaling, whereas hCI2+EN2 and CISD+EN2 scale as $O(N^8)$, though with a small prefactor stemming from the EN2 calculation, which employs a very efficient semistochastic algorithm.[96] The computational scaling associated with the CI+EN2 calculations is also presented in Table I.

To gauge the performance of hCI, eCI, and sCI for radicals, we calculated the ground-state potential energy curves (PECs) for the dissociation of four radicals: OH, CN, vinyl (C_2H_3), and H_7. The CI calculations employed the ground-state restricted open-shell HF orbitals, described with the cc-pVDZ basis set and within the frozen-core approximation. For such small systems and basis sets, FCI is attainable and provides the reference results for gauging the approximate CI models. The equilibrium geometry of vinyl was taken from ref 98 and is also reproduced in the Supporting Information. Their PECs were computed along the C═C double bond breaking coordinate, with the remaining internal coordinates kept frozen. For H_7, we considered equally spaced and linearly arranged hydrogen atoms, and the PECs were computed along the symmetric dissociation coordinate.

The results were analyzed along the same lines as our previous report on hCI for closed-shell systems.[10] Namely, for the different CI models considered here, we evaluated the convergence of the nonparallelity error (NPE), the distance error, the harmonic vibrational frequencies, and the equilibrium bond lengths as functions of N_{det}. The NPE of a given level of theory is defined as the maximum minus the minimum energy difference between its corresponding PEC and the FCI PEC for a given range of coordinates. Here we redefine the previous definition of the distance error[10] to account for the fact that the approximate PEC might appear below the FCI one when perturbative corrections are employed. In such cases and with the previous definition, undesired negative values could be attained. The distance error is redefined based on the signed differences between two PECs, as the absolute value of their maximum difference plus the absolute value of their minimum difference, evaluated at a given coordinate interval. This new definition measures how close two PECs are, remaining always non-negative. From here on, we employ equilibrium properties when referring to both the equilibrium geometry and the harmonic vibrational frequency. Details about how the

https://doi.org/10.1021/acs.jctc.3c00946
J. Chem. Theory Comput. 2023, 19, 8654−8670

equilibrium properties were obtained from the calculated PECs, along with the ranges defining the NPE and distance errors, can be found in the Supporting Information.

The various CI models introduced here were further assessed based on calculated vertical excitation energies for 69 electronic states from 17 closed-shell systems and 13 radicals (shown in Table II), with geometries extracted from the QUEST database.[99] Our set includes mostly small systems, ranging from BH to glyoxal, displaying a mix of valence and Rydberg singly excited states and two doubly excited states (glyoxal and nitroxyl). It does not include large molecules or charge transfer states. The full set of excited states and calculated excitation energies for the various CI models are provided in the Supporting Information.

Table II. Systems Considered in the Excited-State Calculations

closed shells			open shells		
glyoxal	HCF	H_2O	BeH	NH_2	HCO
acetaldehyde	HCCl	H_2S	BeF	PH_2	HOC
silylidene	HPO	N_2	BH_2	vinyl	OH
nitroxyl	CF_2	NH_3	CN	allyl	CO^+
ethylene	BH	HCl	CH_3		
methanimine	BF				

We employed the aug-cc-pVDZ basis set for systems having up to three non-hydrogen atoms and the 6-31+G(d) basis set for the larger ones. Core orbitals were frozen systematically. We impose the CI solutions to be eigenstates of the spin angular momentum operator, which implies accounting for a set of appropriate spin-flipped determinants stemming from higher-order excitations or hierarchies.[90] In this sense, our CIS calculations for radicals actually correspond to the so-called extended CIS[91] for instance, and equivalently for the other hCI, eCI, and sCI models. Notice that spin-contaminated solutions would have energies different from those of the spin eigenstates considered here.

We performed calculations following both the standard ground-state-based CI route and the state-specific CI route.[29] For the latter, we employed the state-specific orbitals obtained in ref 29. Notice that in contrast to eCI, the energies obtained with

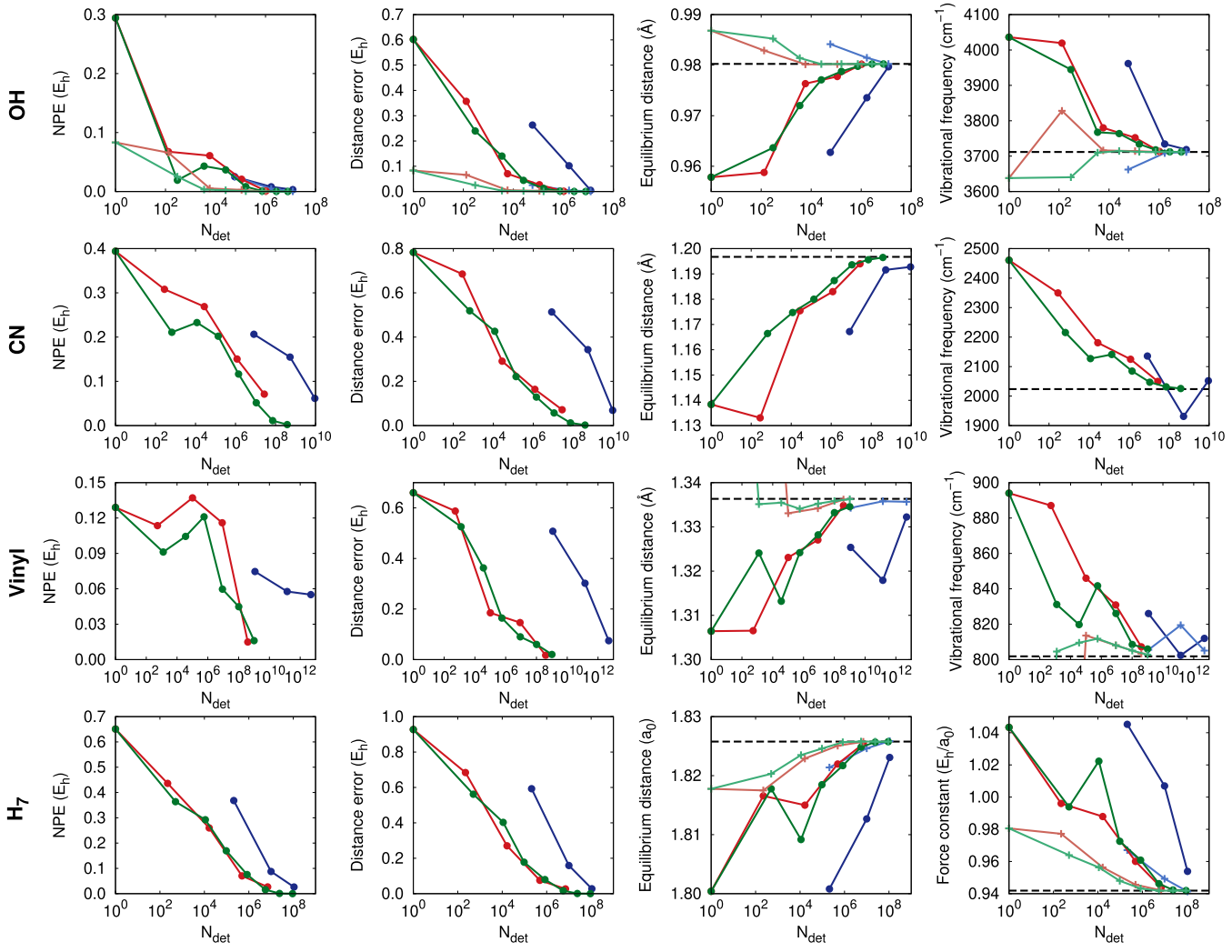

Figure 3. Nonparallelity error (NPE), distance error, equilibrium distance, and vibrational frequency (or force constant) for OH, CN, vinyl, and H_7 as functions of the number of determinants (N_{det}) according to the hCI (green), eCI (red), and sCI (blue) routes, with (light-tone crosses) and without (dark-tone circles) the standard EN2 perturbative correction. Each point denotes one CI model according to the sequences HF, hCI1, hCI1.5, hCI2, etc. (green); HF, CIS, CISD, etc. (red); and sCI1, sCI3, and sCI5 (blue). The dashed lines represent the FCI results.

https://doi.org/10.1021/acs.jctc.3c00946
J. Chem. Theory Comput. 2023, 19, 8654−8670

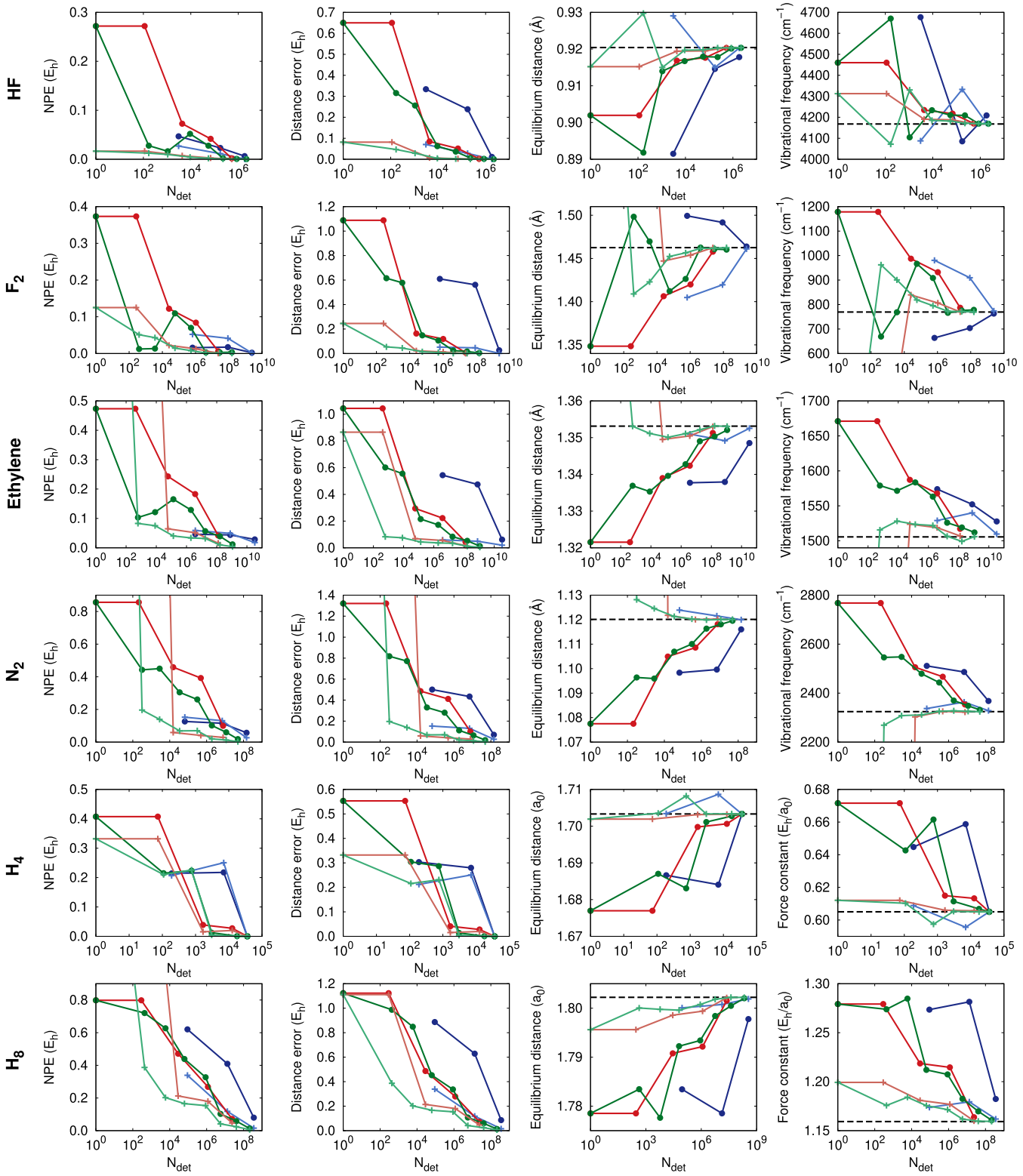

Figure 4. Nonparallelity error (NPE), distance error, equilibrium distance, and vibrational frequency (or force constant) for HF, F_2, ethylene, N_2, H_4, and H_8 as functions of the number of determinants (N_{det}) according to the hCI (green), eCI (red), and sCI (blue) routes, with (light-tone crosses) and without (dark-tone circles) the standard EN2 perturbative correction. Each point denotes one CI model according to the sequences HF, hCI1, hCI1.5, hCI2, etc. (green); HF, CIS, CISD, etc. (red); and sCI0, sCI2, and sCI4 (blue). The dashed lines represent the FCI results.

the sCI and hCI models are not invariant under rotations within the occupied and virtual subspaces. The restricted HF solution (restricted open-shell HF for the open-shell systems) was taken as the reference determinant for the hCI and eCI ground-state calculations (left and middle panels of Figure 1). For the state-specific hCI and eCI calculations, we employed a minimal CSF reference:[29] a single open-shell determinant for the doublet excited states and a single open-shell CSF for the excited states

https://doi.org/10.1021/acs.jctc.3c00946
J. Chem. Theory Comput. 2023, 19, 8654−8670

from closed-shell systems (middle and right panels of Figure 1, respectively). The computed excitation energies were benchmarked against the reference theoretical values provided in the QUEST database.[99] For each excited state considered here, the reference value and the method used to obtain it (of high-order CC or extrapolated FCI quality) can be found in the Supporting Information.

For the sCI models, we considered sCI1 for both ground- and (state-specific) excited-state calculations for the doublet open-shell systems. For the closed-shell systems and their excited states, we explored two models. In the sCI2/sCI0 model, the ground state was described with sCI0 and the excited state with sCI2, which is the minimal sCI calculation for computing singly excited states of closed-shell systems. Further including the seniority-two sector for the ground-state calculations defines the sCI2/sCI2 model.

From here on, CI models carrying the Δ symbol denote a state-specific approach, whereas those without it correspond to a ground-state-based approach.

IV. RESULTS AND DISCUSSION

A. hCI for Radicals. The full set of PECs for the open-shell systems (OH, CN, H_7, and vinyl) are presented in the Supporting Information. From these PECs, we obtain the NPEs, distance errors, equilibrium bond lengths, and harmonic vibrational frequencies, which are plotted as functions of N_{det} in Figure 3. Each point in the figure denotes one CI model. For instance, the hCI route is represented by the dark green line, with the first point being hCI0 (which corresponds to HF in the present cases), the second being hCI1, the third being hCI1.5, etc. The corresponding results for the closed-shell systems (HF, F_2, N_2, ethylene, H_4, and H_8) are shown in Figure 4. When we first introduced hCI,[10] we surveyed the same molecules, though only for the bare CI models (without a perturbative correction). These previous results are reproduced in Figure 4 together with the present results, which include such correction. First, we discuss the results for the bare CI models (hCI, eCI, and sCI) for the open-shell systems (represented by the dark tones in the figures), leaving the discussion about the perturbative correction (light tones) for both open-shell and closed-shell systems to section IV B.

We find that hCI typically improves the convergence with respect to N_{det} compared to eCI for the four properties surveyed here. The present finding for open-shell systems therefore parallels the previously reported superiority of hCI for closed-shell systems.[10]

The smaller NPEs obtained with hCI are related to the better description of the PECs at dissociation. This is due to a larger fraction of static correlation being recovered, stemming from the classes of determinants appearing lower in the seniority–excitation map (see Figure 1), namely, determinants high in excitation degree e and low in seniority s, that are absent in eCI of the same order. The smaller NPEs attained with hCI are clear for OH (involving single-bond breaking), vinyl (double-bond breaking), and CN (triple-bond breaking), whereas for H_7 (multiple bond breaking), hCI and eCI are comparable. This dependence on the order of bond breaking had also been observed for closed-shell systems[10] (as can be seen in Figure 4) and would be expected, as describing dissociation becomes increasingly more challenging as the bond order increases. Even though hCI manages to recover more static correlation than eCI, the advantage of the former is more striking for single-bond breaking, whereas multiple bond breaking (such as H_7 and H_8) inevitably requires higher-order excited determinants.

The distance errors obtained with hCI and eCI are overall comparable for open-shell systems, whereas the former presents slightly better convergence for the closed-shell systems. In comparison to eCI, hCI leads to either comparable or somewhat faster (for CN) convergence of the equilibrium geometries for open-shell systems. Finally, hCI systematically outperforms eCI in the calculation of vibrational frequencies, except for H_7, where no big difference is found. For the CN radical, CIS, sCI1, and sCI3 produce crossings between ground and excited states around equilibrium and hence nonsmooth adiabatic PECs and somewhat less reliable equilibrium properties in these specific cases. Given the overall slight superiority of hCI for the equilibrium properties, it also manages to account for more dynamic correlation than eCI for both open-shell and closed-shell systems.

In great contrast to hCI and eCI, sCI models deliver poor convergence of all observables. The single exception is the NPE for OH obtained from sCI0, which is in between the NPEs obtained from hCI2 and CISDT, methods having a computational cost comparable to that of sCI0 in this particular case. Going to larger basis sets or bigger systems, the computational burden of sCI models would increase considerably more than hCI or eCI models due to its formal exponential scaling. As far as configuration interaction methods are concerned, we conclude that the sCI route is unattractive for open-shell systems, in line with similar findings for closed-shell systems[10] (also see Figure 4).

We recall that ground-state restricted open-shell HF orbitals were employed in all calculations for the ground-state radicals. In contrast to eCI, methods that rely on the seniority to generate excited determinants (like the hCI and sCI models addressed here) are not invariant under orbital rotations within the occupied and virtual subspaces.[3,66,74] One could exploit the rotations within each subspace (by means of orbital localization, for example) to hopefully render more suitable orbitals for hCI and sCI calculations. In our first contribution on hCI for closed-shell systems,[10] we went one step further and variationally optimized the orbitals at the correlated CI level, thus allowing rotations between occupied and virtual subspaces. Except for the lower-order CI models, the cost and complications of orbital optimization outweigh the mixed improvement in the computed properties.[10] For the closed-shell systems (surveyed both here and in the previous study[10]), the results become significantly more accurate with the EN2 perturbative correction rather than by variationally optimizing the orbitals.

B. hCI Plus EN2 Correction. The results for the CI models corrected by the standard EN2 energy are represented by the light tones in Figures 3 and 4. We excluded instances where the PECs present important discontinuities. These discontinuities reflect crossings between states of different symmetries in the unperturbed CI calculation, appearing as kinks in the computed ground-state PEC. Due to the abrupt change of character, the EN2 correction is not uniform and gives rise to the observed discontinuities. This happens for the open-shell systems at dissociation (except for OH), for which we do not present NPEs or distance errors. For OH and the six closed-shell systems, the EN2 correction produced smooth PECs at dissociation. Around the equilibrium geometry, the EN2 correction also leads to well-behaved PECs for all CI models and for all systems except for CN (thus, no equilibrium properties are presented for this radical). This is simply due to its several close-lying excited

https://doi.org/10.1021/acs.jctc.3c00946
J. Chem. Theory Comput. 2023, 19, 8654−8670

states. If we were to follow the PEC of a given symmetry (and not the lowest-lying state as we did here), then there would be no discontinuities stemming from the EN2 contribution.

We found that the EN2 perturbative correction significantly reduces the errors in the bare CI calculations. This is observed for all of the CI models, systems, and observables considered here. For OH, in particular, the improvement is massive, as even the lower levels of CI+EN2 deliver very close results to those of FCI. Importantly, the hCI+EN2 route outperforms its eCI+EN2 counterpart, thus preserving the advantage observed without the perturbative correction. Similarly, the correction typically maintains a comparable performance of the two routes when this is the case according to the unperturbed CI calculations.

The improvement brought by the perturbative correction is such that a given CI+EN2 model often provides more accurate results than the higher-order bare CI model sharing the same computational scaling. For instance, hCI1+EN2 and hCI2 display the same $O(N^6)$ computational scaling, and the former outperforms the latter in many cases. In Figures 3 and 4, hCI1+EN2 correlates with the second light-green mark and hCI2 with the fourth dark-green mark. The former model provides smaller NPEs and distance errors for OH, HF, and F_2 (all single-bond breakings), the opposite being true for multiple bond breaking. The advantage of the EN2 correction is more striking for the equilibrium properties, where hCI1+EN2 is more accurate than hCI2 for OH, vinyl, ethylene, and N_2, whereas the two models perform similarly for the remaining systems. It is worth recalling that the prefactor associated with the EN2 calculation is smaller than the one associated with the higher-order CI calculation, which in the above example makes hCI1+EN2 cheaper than hCI2. In many cases, the accuracy of hCI1+EN2 is actually better than or comparable to that of hCI2.5 or CISDT, which are considerably more expensive models.

A similar impact on the effect of the EN2 correction also holds for eCI. For that, we compare CISD+EN2 and CISDT, both of which show $O(N^8)$ scaling. CISD+EN2 correlates with the third dark-red mark and CISDT with the fourth light-red mark in Figures 3 and 4. The errors for the four observables are systematically smaller than those of the former model, except for the NPE and distance error of H_8 and the equilibrium properties of H_7, where they are comparable.

The EN2 correction usually ameliorates the performance of the sCI route, though to a lesser extent than observed for hCI and eCI. This reflects the poorer reference provided by sCI, from which perturbation theory struggles to recover. In a handful of cases, the EN2 correction does not improve the bare sCI results for both NPEs (OH, N_2, F_2, and ethylene) and equilibrium properties (vinyl, HF, F_2, and ethylene). Overall, the sCI+EN2 route is too expensive for the attained accuracy.

In very few cases, the EN2 correction does not improve the bare CI results, suggesting an important cancellation of errors in the latter. This is seen when employing the hCI1 and hCI1+EN2 models to compute the NPE of OH and F_2 and to some extent the equilibrium properties of F_2. These are exceptions, though, as the EN2 correction practically always improves the accuracy of the computed observables. It further leads to an overall more monotonic convergence of the observables. In this sense, it regularizes oscillations seen in the unperturbed case, probably related to the cancellation of errors at lower orders. This is clearly seen in the equilibrium properties of vinyl, H_7, and F_2 and in the NPE of OH, HF, F_2, and ethylene.

Instead of the usual EN2 correction discussed so far and shown in Figures 3 and 4, one can compute the renormalized EN2 correction.[64] Analogous results showing the convergence of observables for both usual and renormalized EN2 corrections are listed in the Supporting Information. Significant differences can be encountered at the lower orders of CI, becoming negligible at higher orders. More often than not, the usual correction performs better. The difference is noticeable for ethylene, N_2, H_7, and H_8 and to a lesser extent for vinyl, whereas for H_4 the results are mixed. The renormalized correction is slightly more accurate for OH, HF, and F_2. These results suggest that renormalizing the EN2 energy may be helpful only for single-bond breaking, though by a small amount, whereas it worsens the results for multiple bond breaking. Overall, the usual EN2 correction should probably be favored when employed in combination with the approximate CI models.

We further explored hCI to describe the automerization barrier in the ground state of cyclobutadiene, which connects the two equivalent rectangular D_{2h} equilibrium geometries through the square D_{4h} transition state geometry.[100,101] This is a well-known and challenging problem, requiring high-level calculations to achieve quantitative values for the height of the barrier (see ref 89 and references therein). Here we employ the geometries presented in ref 89, the 6-31+G(d) basis set, and the frozen-core approximation. We optimize the orbitals for two closed-shell determinants in the D_{2h} geometry and for two spin-flipped open-shell determinants in the D_{4h} geometry, from which the excited determinants were generated in the subsequent CI calculations. Even though the calculations target the ground state, they are labeled ΔCI because different references are employed for each geometry. For this basis set, the reference value of 7.51 kcal/mol was obtained using CC with single, double, triple, and quadruple excitations.[89] With respect to this reference value, the errors for the automerization barrier are 3.55 kcal/mol with our two-determinant calculations, −2.28 kcal/mol with ΔhCI2, −1.07 kcal/mol with ΔhCI2+EN2, 0.61 kcal/mol with ΔCISD, and −0.49 kcal/mol with ΔCISD+EN2. These values are comparable to those obtained with other methods, extensively discussed in ref 89. Here we just mention the errors of CC with singles and doubles, 0.80 kcal/mol, and of spin-flip equation-of-motion CC (EOM-CC) with singles and doubles, −1.65 kcal/mol, which share the same $O(N^6)$ computational scaling as ΔCISD and ΔhCI2. This specific example serves to illustrate that the accuracy of hCI models can be similar to that of other methods. As such, hCI can be taken into consideration in future systematic studies that tackle challenging chemical problems in which strong correlation comes into play.

C. hCI for Excited States. For each CI model considered here, we evaluate the mean signed error (MSE), mean absolute error (MAE), root-mean-square error (RMSE), and standard deviation of the errors (SDE) with respect to the reference theoretical values for the excitation energies. For completeness, the definition of these statistical measures can be found in the Supporting Information. For the lower-order models, calculations were performed for 50 (closed-shell) and 19 (open-shell) excited states. In turn, subsets of 16 (closed-shell) and six (open-shell) excited states were considered for the higher-order CI models, given the more intensive computational cost. Even though these subsets are too small for meaningful absolute statistics, they should be enough to reveal the main trends. A detailed comparison of eCI based on ground-state and state-specific approaches can be found elsewhere.[29] The focus of the

https://doi.org/10.1021/acs.jctc.3c00946
J. Chem. Theory Comput. 2023, 19, 8654−8670

Table III. Mean Signed Error (MSE), Mean Absolute Error (MAE), Root-Mean Square Error (RMSE), and Standard Deviation of the Errors (SDE) (in eV) with Respect to Reference Theoretical Values for the Set of Singly Excited States of Closed-Shell Systems Listed in the Supporting Information

method	count	MSE	MAE	RMSE	SDE	method	count	MSE	MAE	RMSE	SDE
CIS	48	+0.03	0.61	0.59	0.77						
CISD	16	+4.09	4.09	4.18	0.84						
CISDT	16	+0.12	0.17	0.18	0.14						
CISDTQ	16	+0.15	0.15	0.17	0.08						
hCI1	50	+1.07	1.16	1.39	0.89	hCI1+EN2	50	+0.65	0.65	0.84	0.53
hCI1.5	50	+1.95	1.95	2.04	0.59	hCI1.5+EN2	50	+0.62	0.63	0.76	0.44
hCI2	16	+2.99	3.53	3.61	0.76						
hCI2.5	16	+1.95	1.95	2.06	0.66						
hCI3	16	+0.19	0.19	0.21	0.08						
hCI3.5	16	+0.11	0.11	0.13	0.07						
ΔCSF	50	−0.71	0.77	0.91	0.58						
ΔCISD	50	−0.12	0.17	0.22	0.18	ΔCISD+EN2	50	+0.02	0.06	0.09	0.09
ΔCISDT	16	−0.20	0.20	0.22	0.11						
ΔCISDTQ	16	−0.02	0.02	0.02	0.02						
ΔhCI1	50	−1.40	1.40	1.55	0.67	ΔhCI1+EN2	50	+0.12	0.24	0.30	0.27
ΔhCI1.5	50	−2.80	2.80	3.03	1.15	ΔhCI1.5+EN2	50	−0.01	0.13	0.19	0.19
ΔhCI2	50	−0.18	0.20	0.25	0.16	ΔhCI2+EN2	50	+0.01	0.07	0.10	0.10
ΔhCI2.5	16	−0.27	0.27	0.30	0.13						
ΔhCI3	16	−0.22	0.22	0.24	0.10						
ΔhCI3.5	16	−0.08	0.08	0.09	0.05						
sCI2/sCI2	50	+1.35	1.35	1.51	0.68	sCI2/sCI2+EN2	50	+0.60	0.60	0.79	0.51
sCI2/sCI0	50	−0.34	0.55	0.74	0.66	sCI2/sCI0+EN2	50	+0.51	0.52	0.69	0.47
ΔsCI2/sCI2	50	+0.66	0.78	0.89	0.60	ΔsCI2/sCI2+EN2	50	+0.21	0.26	0.35	0.28
ΔsCI2/sCI0	50	−1.04	1.04	1.21	0.62	ΔsCI2/sCI0+EN2	50	+0.12	0.23	0.27	0.24

present discussion lies on the comparison of hCI with eCI and sCI and on a similar comparison between ground-state and state-specific approaches for hCI and sCI. The bare (unperturbed) hCI and sCI models are discussed in this section and in section IV D, respectively, whereas their EN2-perturbed analogues are left for section IV E.

We start the discussion with the excitations from closed-shell systems with the corresponding statistical errors shown in Table III. The first level of hCI, hCI1, produces poor excitation energies, with a MAE of 1.16 eV. This model has the same computational scaling as CIS but includes the paired double excitations, which clearly worsen the decent CIS results (MAE of 0.61 eV). Moving one rank up, to hCI1.5, the MAE increases to 1.95 eV, and then it reaches a maximum of 3.53 eV at the hCI2 level. We notice that hCI2 delivers somewhat smaller errors than CISD (MAE of 4.09 eV), even though both are way too large. From that point on, the next hCI models generate progressively better results. Despite the improvement with respect to hCI2, hCI2.5 is still as inaccurate (MAE of 1.95 eV) as hCI1.5. At the hCI3 level, significantly smaller errors are finally achieved (MAE of 0.19 eV). This is close to that obtained with the eCI model of the same order, CISDT (0.17 eV). Even smaller errors are produced at the hCI3.5 level (MAE of 0.11 eV), but at a considerable computational cost.

As discussed above, the errors in excitation energies obtained with the hCI models first increase as one augments the hierarchy parameter h, reaching a maximum at hCI2, and then decrease toward higher orders. This behavior parallels what is well-established for the excitation energies computed with eCI, where CISD is far worse than CIS, which in turn is inferior to CISDT, whereas CISDTQ is considerably more accurate. This can be understood based on the role of the excited determinants for ground and excited states. The excited determinants of the low-order hCI models (hCI1 and hCI1.5) already account for some correlation for the ground state but represent mostly orbital relaxation of the excited state, which thus remains less correlated. This favored description of the ground state explains the overestimated excitation energies at these orders. The effect becomes exaggerated at the hCI2 (and CISD) level since it captures most of the ground state correlation through the unpaired double excitations, which in turn just start to describe correlation for the excited state. Higher-order models, starting at hCI3 and CISDT, are needed to recover a large fraction of the excited-state correlation, and at this point the errors in the excitation energies decline progressively. Because the excited determinants are accessed from the ground-state determinant and are due to ground-state HF orbitals, the description of the ground state is always favored. This explains why hCI systematically overestimates the excitation energies, just as eCI does.

Employing state-specific orbitals would be expected to suppress the bias toward the ground state and lead to improved results, as observed, for instance, when going from CISD to ΔCISD.[29] However, for the low orders of state-specific hCI (ΔhCI1 and ΔhCI1.5), we actually found larger errors than with the ground-state-based approach, this time by underestimating the excitation energies. Besides the set of orbitals, the classes of determinants included at each order play an equally important role and explain our observation. Still considering the excitations of the closed-shell systems, different classes of determinants are accessed from the ground-state reference (a closed-shell determinant) and from the excited-state reference (a single open-shell CSF) for a given hierarchy parameter h. The case of ΔhCI1 can be understood by comparing the hCI1 determinants for these two references, as shown in Figure 2. There is far more diversity in the classes of determinants employed for the excited-

https://doi.org/10.1021/acs.jctc.3c00946
J. Chem. Theory Comput. 2023, 19, 8654−8670

Table IV. Mean Signed Error (MSE), Mean Absolute Error (MAE), Root-Mean Square Error (RMSE), and Standard Deviation of the Errors (SDE) in Units of eV, with Respect to Reference Theoretical Values, for the Set of Singly-Excited States from Open-Shell Doublets Listed in the Supporting Information

method	count	MSE	MAE	RMSE	SDE	method	count	MSE	MAE	RMSE	SDE
CIS	19	+0.38	0.41	0.63	0.50						
CISD	6	+2.97	2.97	3.19	1.17						
CISDT	6	+0.06	0.07	0.09	0.06						
CISDTQ	6	+0.08	0.08	0.11	0.08						
hCI1	19	+0.65	0.73	0.91	0.64	hCI1+EN2	19	+0.27	0.28	0.36	0.24
hCI1.5	19	+1.07	1.07	1.26	0.68	hCI1.5+EN2	19	+0.22	0.25	0.33	0.24
hCI2	6	+1.32	1.32	1.60	0.90						
hCI2.5	6	+0.03	0.05	0.06	0.05						
hCI3	6	+0.00	0.04	0.05	0.05						
hCI3.5	6	+0.01	0.03	0.05	0.04						
ΔCSF	19	−0.04	0.43	0.59	0.59						
ΔCISD	19	+0.00	0.12	0.21	0.21	ΔCISD+EN2	19	−0.02	0.04	0.06	0.06
ΔCISDT	6	−0.07	0.07	0.10	0.08						
ΔCISDTQ	6	−0.02	0.02	0.02	0.02						
ΔhCI1	19	−0.21	0.35	0.49	0.44	ΔhCI1+EN2	19	+0.02	0.17	0.29	0.29
ΔhCI1.5	19	−0.14	0.45	0.70	0.69	ΔhCI1.5+EN2	19	+0.00	0.10	0.15	0.15
ΔhCI2	19	−0.02	0.10	0.16	0.16	ΔhCI2+EN2	19	−0.00	0.05	0.08	0.08
ΔhCI2.5	6	−0.09	0.09	0.14	0.10						
ΔhCI3	6	−0.06	0.06	0.08	0.05						
ΔhCI3.5	6	−0.02	0.02	0.03	0.02						
sCI1	19	+0.20	0.35	0.57	0.53	sCI1+EN2	19	+0.23	0.25	0.32	0.21
ΔsCI1	19	−0.12	0.28	0.39	0.37	ΔsCI1+EN2	19	+0.06	0.12	0.20	0.19

state calculation than for the ground-state one, a consequence of the different references. Because of that, low orders of hCI may be expected to capture a larger fraction of correlation for the excited state than for ground state. This is further supported by the more accurate results obtained for excitations of open-shell systems (discussed in detail later), where the same type of reference is employed. Although hCI is constructed to account for all classes of determinants whose number share the same computational scaling, at the lower orders this procedure does not lead to a balanced description of correlation, at least for excitations of closed-shell systems and the present choice of minimal references. An important point to realize from the present results is that a state-specific approach is not necessarily more accurate than a ground-state-based approach. Both the orbitals and the classes of determinants of a given CI model control the fine balance of ground- and excited-state correlation effects.

At the ΔhCI2 level, the imbalance associated with the state-specific classes of determinants is reduced to a great extent. At this level, the state-specific advantage clearly manifests, with ΔhCI2 having a MAE of 0.20 eV, which is substantially smaller than the MAE of 3.53 eV obtained from hCI2. This comparison between ground-state-based and state-specific approaches is analogous to our previous finding on the eCI models of the same order, CISD, and ΔCISD.[29] Even though hCI2 is somewhat more accurate than CISD (both have large errors), their state-specific versions share comparable performance. Actually, ΔhCI2 is slightly less accurate than ΔCISD, with MAEs of 0.20 and 0.17 eV. Moreover, ΔhCI2 has a more negative MSE than ΔCISD (−0.18 eV against −0.12 eV). Albeit small, these differences are statistically significant, and ΔCISD would still be preferable to ΔhCI2 by some margin. The slightly worse performance of ΔhCI2 probably stems from a residual imbalance associated with the state-specific classes of determinants. ΔhCI2 is more accurate for singlets than for triplets (MAEs of 0.16 and 0.25 eV), whereas Rydberg states are better described than valence states (MAEs of 0.14 and 0.24 eV). The same trends are found for the low-order models (ΔhCI1 and ΔhCI1.5) and also for ΔCISD, which slightly outperforms ΔhCI2 for each type of excitation. The specific MAEs can be found in the Supporting Information.

Moving to ΔhCI2.5 increases the errors (MAE of 0.27 eV) compared to ΔhCI2 (MAE of 0.20 eV). This could be due to another set of unbalanced state-specific determinants that enters at this stage, like what was observed between ΔhCI1 and ΔhCI1.5. Despite the differing number of states considered, the observed variation in the accuracy of ΔhCI2 and ΔhCI2.5 is statistically significant, which is confirmed by calculating the statistical errors for the same subset of excited states. Even though ΔhCI2.5 is much more accurate than hCI2.5, ΔhCI2 or ΔCISD remains cheaper and more accurate.

The situation improves at ΔhCI3 (MAE of 0.22 eV), though it still remains less accurate than ΔhCI2, which is only surpassed at the ΔhCI3.5 level (MAE of 0.08 eV). There is no gain in going from hCI3 (MAE of 0.19 eV) to ΔhCI3 and from hCI3.5 (MAE of 0.11 eV) to ΔhCI3.5, like what had been found for CISDT and ΔCISDT.[29] We notice, however, that the state-specific route presents negative MSEs, in contrast to the positive values obtained with the ground-state-based route for both hCI and eCI. Furthermore, eCI and hCI present comparable performances at this order, with an arguable preference for the former, as also discussed above for ΔCISD and ΔhCI2.

We now shift to a discussion of excitations for open-shell systems. The statistical errors are shown in Table IV. The key difference in the calculations for open-shell excitations is that the same type of reference was employed for ground- and excited-state calculations, namely, a single open-shell determinant, shown in the center panel of Figure 1. In contrast, the excited states from the closed-shell systems relied on different classes of reference determinants. This accounts for the more accurate

https://doi.org/10.1021/acs.jctc.3c00946
J. Chem. Theory Comput. 2023, 19, 8654−8670

results observed for open-shell excitations and explains most of the differences with respect to excitations from closed-shell systems, as discussed in detail in the following.

When using ground-state orbitals, we found that the performance initially degrades and later improves as the order increases, for both eCI and hCI. This is similar to what was observed for the closed-shell excitations and can be traced back to a biased description of the ground state related to the choice of ground-state orbitals. An important difference, however, is that the maximum error, also at hCI2, is significantly smaller (MAE of 1.32 eV) for open shells than for closed shells (MAE of 3.53 eV). This clearly reflects the choice of reference, as both the ground and excited states of the open shells considered here are qualitatively described with the same type of determinant. For the same reason, the MSEs are systematically smaller for the open-shell excitations (though still positive because of the ground-state orbitals).

Once state-specific orbitals are employed, there is no remaining bias toward the ground state. In stark contrast to the closed-shell case, the lower orders of ΔhCI, ΔhCI1 (MAE of 0.35 eV) and ΔhCI1.5 (MAE of 0.45 eV), become more accurate than their ground-state-based counterparts, hCI1 (MAE of 0.73 eV) and hCI1.5 (MAE of 1.07 eV). Once again, this is thanks to the same type of reference in ground- and excited-state calculations. The case of ΔhCI1 for open-shell excitations is depicted in Figure 2, in comparison to the more unbalanced case of excitations from closed shells. We notice, however, an apparent residual bias from the somewhat negative MSEs (−0.21 eV with ΔhCI1 and −0.14 eV with ΔhCI1.5) and that ΔhCI1.5 is slightly less accurate than ΔhCI1.

This residual bias virtually disappears at the next order, ΔhCI2 (MSE of −0.02 eV), whereas for the closed-shell systems even ΔhCI3.5 significantly underestimated the excitation energies (MSE of −0.08 eV). The same comparison between open and closed shells holds true for eCI models. For the open-shell transitions, ΔhCI2 is slightly more accurate (MAE of 0.10 eV and RMSE of 0.16 eV) than ΔCISD (MAE of 0.12 eV and RMSE of 0.21 eV). In further contrast to the closed-shell case, ΔhCI2.5 is as accurate as ΔhCI2, producing a MAE of 0.09 eV. (Accounting only for the six states considered for ΔhCI2.5, ΔhCI2 would also have a MAE of 0.09 eV.) Likewise, higher-order hCI models are progressively more accurate. Even though the statistics become more limited, they suggest both a small advantage of the hCI models against eCI and that the ground-state routes perform slightly better than the state-specific ones.

For the state-specific models, we have further assessed the impact of not imposing spin eigenstates (the results and statistics can be found in the Supporting Information). This amounts to not including the appropriate spin-flip determinants lying above the hierarchy or excitation degree of choice. The effect is minimal for the excitation energies of both closed- and open-shell systems in the ΔhCI1.5, ΔhCI2, and ΔCISD models. The mean difference on the individual excitation energies lies between 0.01 and 0.02 eV for the latter two and 1 order of magnitude less for ΔhCI1.5. Similarly, small effects are seen in the global statistics. In turn, ΔhCI1 is more affected, which would be expected since it is a low-order model. Average individual excitations of closed- and open-shell systems vary by 0.26 and 0.06 eV, respectively, always in the sense of improving the energies in the former case, though not enough to cause a considerable reduction of the large absolute errors. Overall, not constraining the CI solutions to have well-defined spin brings practical complications (as more roots have to be calculated) and does not improve the computed excitation energies obtained with the more competitive ΔCISD and ΔhCI2 models. The sCI models, discussed in the next subsection, are naturally spin eigenstates, and there is no need to enforce that.

D. sCI for Excited States. We refer back to Table III to discuss the performance of sCI for excited states of closed-shell systems. The first model, sCI2/sCI2, systematically overestimates the excitation energies, producing a MAE of 1.35 eV. The same two factors discussed above for hCI explain such large errors. First, the ground-state description is favored due to the use of ground-state HF orbitals. Indeed, with state-specific orbitals, the ΔsCI2/sCI2 model reduces the MAE to 0.78 eV, although still overestimating the excitation energies. Second, there is an unbalanced description of the correlation for ground and excited states, associated with the classes of determinants. While sCI2/sCI2 accounts for an additional $s = 2$ sector for the ground state (which can be qualitatively described in the $s = 0$ sector), no additional pairs of electrons are allowed to become unpaired in the excited state calculation, even though the state is qualitatively described by a determinant that is contained in the $s = 2$ sector. In other words, unpaired excitations are allowed to correlate the ground state but not the excited state, given their respective closed-shell and open-shell characters, thus creating a bias toward the former.

A possible solution to this imbalance is to restrict the determinants to a maximum seniority number of $s = 0$ for the ground-state and $s = 2$ for the excited-state calculation. This is precisely the sCI2/sCI0 model, which delivers a MAE of 0.55 eV, compared to 1.35 eV for sCI2/sCI2. However, when going to state-specific orbitals, ΔsCI2/sCI0 systematically undershoots the excitation energies and provides a MAE of 1.04 eV. Clearly, the seniority-two sector captures more correlation for the excited states than does the seniority-zero for the ground state. Ultimately, we did not find a combination of sCI models and orbitals that produced reasonable excitation energies for closed-shell systems.

The situation for open-shell systems is quite different, in close analogy to the previous discussion regarding hCI. As shown in Table IV, sCI1 provides considerably more accurate excitation energies for open-shell systems than for closed-shell systems. The reason should not be surprising at this point. Both ground and excited states of open shells can be qualitatively described by the same type of reference (a single $s = 1$ open-shell determinant). Moreover, the state-specific approach is superior. sCI1 presents a MAE of 0.35 eV and overestimates the excitation energies (MSE of 0.20 eV) in view of the bias introduced by the ground-state orbitals. With state-specific orbitals, ΔsCI1 reduces the MAE to 0.28 eV and the MSE to −0.12 eV, which is smaller in absolute value than found for sCI1.

Even though ΔsCI1 is less accurate and has less favorable computational scaling than CI models like ΔCISD and ΔhCI2, its decent errors are encouraging for another reason: the development of polynomial-scaling CC methods based on the concept of seniority. For closed-shell systems, DOCI (here referred to as sCI0) energies can be very well reproduced with state-specific pair coupled-cluster doubles (pCCD), a method that has mean-field cost for both ground[3−6] and excited[60,61] states. Likewise, a formulation of pCCD for open-shell systems might share an analogous connection to low-order sCI models like sCI1. If that is the case, then a state-specific approach for such a pCCD formulation adapted to open shells may approach the accuracy of ΔsCI1 (MAE of 0.28 eV) at a mean-field cost. This method could then provide an improved starting point to

https://doi.org/10.1021/acs.jctc.3c00946
J. Chem. Theory Comput. 2023, 19, 8654−8670

recover the remaining weak correlation compared to starting from the (also mean-field though less accurate) ΔCSF model (MAE of 0.43 eV). To the best of our knowledge, there has been a single proposed extension of pCCD to open-shell systems,[78] based on the ionization-potential equation-of-motion CC (EOM-CC) formalism.[102−104]

As pointed out previously, hCI and sCI models are not invariant under rotations within the subspaces of occupied and virtual orbitals. For the state-specific calculations, such rotations for the excited-state orbitals represent additional degrees of freedom to those of the ground-state orbitals.[10] As discussed at the end of section IV A, these degrees of freedom could be exploited by localizing occupied and virtual subspaces or by variationally optimizing all orbitals at a correlated level, for instance. We did not pursue these ideas here, and their impact on the excitation energies computed with hCI and sCI remains an open question.

E. hCI and sCI Plus EN2 Correction for Excited States.

The renormalized EN2 correction significantly reduces the errors across most CI models for both closed- and open-shell systems. The statistical measures for the CI models corrected with the EN2 correction can be seen in Table III (closed-shell systems) and Table IV (open-shell systems), along with the results for the bare (unperturbed) CI models. We did not consider the EN2 correction for the higher-order models.

For a given scaling (see Table I), whether the bare CI model or the lower-order CI model plus EN2 correction produces the smaller errors depends on the truncation order and also on the type of excitations (from closed or open shells). For instance, ΔhCI2 and ΔhCI1+EN2 have the same $O(N^6)$ computational cost, but the former has smaller MAEs for closed shells (0.20 eV compared to 0.24 eV) and, more significantly, for open shells (0.10 eV compared to 0.17 eV). In turn, ΔhCI1.5+EN2 is significantly more accurate than ΔhCI2.5 for closed shells, with MAEs of 0.13 and 0.27 eV, whereas for open shells both models produce a MAE of 0.10 eV. The same trend is found at the next order. ΔhCI2+EN2 is much more accurate than ΔhCI3 for closed shells, with MAEs of 0.06 and 0.22 eV, whereas for the open-shell transitions, they deliver comparable MAEs of 0.05 to 0.06 eV. We recall that the calculation of the EN2 correction has a small associated prefactor, which makes the above ΔhCI+EN2 models attractive alternatives to their higher-order unperturbed ΔhCI counterparts.

Among the different CI models, it is worth highlighting the huge improvement observed from ΔhCI1.5 to ΔhCI1.5+EN2. For the closed shells, the MAE drops from 2.80 to 0.13 eV, whereas a reduction from 0.45 to 0.10 eV is seen for the open shells. In both cases, the MSE is virtually zero. In addition, the individual errors for singlet, triplet, Rydberg, and valence states are comparable, lying in the range 0.11 to 0.15 eV.

We found a similar impact of the EN2 correction for ΔCISD and ΔhCI2. As discussed above, ΔCISD is somewhat more accurate than ΔhCI2 for the closed shells (MAEs of 0.17 and 0.20 eV), whereas the EN2 correction decreases their respective MAEs to 0.06 and 0.07 eV. In turn, while ΔCISD is slightly less accurate than ΔhCI2 for the open shells (MAEs of 0.12 and 0.10 eV), the EN2-corrected models show MAEs of 0.04 and 0.05 eV, respectively. Furthermore, the accuracy of ΔhCI2+EN2 is comparable for singlets and triplets (MAEs of 0.07 and 0.06 eV) and superior for Rydberg states compared to valence states (MAEs of 0.04 and 0.08 eV). ΔCISD+EN2 displays the same trends, slightly outperforming ΔhCI2+EN2 for each of the four types of transitions mentioned above, just as discussed above for the unperturbed case.

In contrast to the eCI and hCI routes, the EN2 correction has a more limited effect on the sCI route. There is little to no advantage to the models based on ground-state HF orbitals. The outcome is more favorable with state-specific orbitals, where, for the closed shells, ΔsCI2/sCI2+EN2 and ΔsCI2/sCI0+EN2 show comparable MAEs (0.26 and 0.23 eV, respectively). For the open shells, the MAE decreases from 0.28 eV (ΔsCI1) to 0.12 eV (ΔsCI1+EN2), the latter error being comparable to that of the much less expensive ΔhCI1.5+EN2 model (0.10 eV). Despite the improvement, the EN2 correction is not enough to render the sCI models competitive.

V. CONCLUSION

Here we have generalized hCI[10] to an arbitrary reference determinant, thus extending its applicability to radical species and state-specific excited-state calculations.

By surveying the dissociation of four radicals, we found that the hCI route outperforms or matches the eCI route for both weakly correlated (equilibrium properties) and strongly correlated (dissociation) regimes. These and previous[10] findings demonstrate the ability of hCI models to recover weak and strong correlations for both open- and closed-shell systems. Meanwhile, sCI leads to far less accurate results in comparison to hCI or eCI for a given computational cost. For closed- and open-shell systems, the EN2 perturbative correction substantially accelerates and stabilizes the convergence of hCI and eCI (while keeping the advantage of the former), though it ameliorates the sCI route to a lesser extent. The standard EN2 correction typically produced more accurate results than its renormalized form, except perhaps for describing single-bond breaking. Overall, lower-order models (such as hCI1+EN2) were found to be fairly accurate given their low computational cost. At a given CI level, the perturbative correction is significantly more effective in recovering the missing correlation energy than variationally optimizing the orbitals.[10] In the future, it may be worth combining orbital optimization at a lower level of hCI[10] with the correction provided by perturbation theory.

We further gauged the performance of hCI to describe excited states of closed- and open-shell systems based on either HF ground-state orbitals or state-specific orbitals. For excitations of closed-shell systems, ΔhCI2 and ΔhCI3 are comparable to their excitation-based counterparts, ΔCISD and ΔCISDT, whereas ΔhCI1, ΔhCI1.5, and ΔhCI2.5 are inaccurate bearing in mind their computational cost. The poor performance at lower orders is ascribed to the different minimal references employed, a single seniority-zero determinant for the ground state and a single seniority-two CSF for the excited state, which introduces a strong bias on the classes of determinants accessed in the hCI calculations. ΔhCI performs significantly better for the doublet transitions when compared with the results for closed shells. In this case, the reference of both ground and excited states comprises the same type of single seniority-one determinant. The advantage of using state-specific orbitals over ground-state ones depends on the choice of reference and the order in which the CI is truncated. When similar references are adopted (as for the doublet transitions), such an advantage is already evident at ΔhCI1. In contrast, for unlike references (as for the closed-shell excitations), the state-specific approach becomes advantageous only at somewhat higher orders (ΔhCI2). The present findings highlight the challenge in describing, on an equal footing, states with qualitatively different characters, in particular ground and

https://doi.org/10.1021/acs.jctc.3c00946
J. Chem. Theory Comput. 2023, 19, 8654−8670

singly excited states of closed-shell systems. In this regard, rotations within occupied and virtual orbitals represent yet another factor worth exploring in the future developments of hCI models. hCI also produced reasonable energies for the automerization barrier of cyclobutadiene. It remains to be seen how these models perform for other strongly correlated systems, larger molecules, and charge transfer excited states.

The accuracy of the CI models is significantly enhanced thanks to the EN2 correction, the case of ΔhCI1.5 for closed shells being the most striking, with the MAE plummeting from 2.80 to 0.13 eV. Low orders of state-specific CI supplemented with a perturbative correction can thus provide a cost-effective option for the computation of excitation energies.

We put forward the interesting perspective of developing hierarchy-based CC (hCC) methods (hCC1, hCC2, ...) along with derived EOM-CC formulations to target excited states (EOM-hCC1, EOM-hCC2, ...). EOM-CC with single and double excitations (EOM-CCSD)[105−108] is very accurate for describing singly excited states,[98,109,110] although it slightly overestimates their excitation energies. In contrast, CISD provides too-large excitation energies,[29,107] even though the CISD and EOM-CCSD methods span the same excited determinants and rely on HF ground-state orbitals. Here we found that hCI2 is more accurate than CISD, despite its large absolute errors. In particular, the overestimated energies are less exaggerated in the former. We ponder whether this improvement would be transferred to EOM-hCC2. Along the same line, it would be interesting to develop and gauge the performance of cheaper methods like EOM-hCC1. Importantly, it is not obvious what the computational scaling of such methods would be. Alternatively, one can envision state-specific hCC methods to target excited states.

Finally, we employed different sCI models to compute the excitation energies of closed- and open-shell systems. Despite the four different models employed for the closed-shell excitations, the results are overall disappointing. For the open-shell transitions, the outcome is more encouraging. Despite the improvement brought about by the EN2 correction, the sCI models remain less accurate and are more expensive than the eCI or hCI options. The relevance of these sCI models lies in their possible connection to CC methods. While this is already established for closed-shell systems (pCCD and DOCI deliver very similar energies),[3−6,60,61] here we raised the question of whether there exists a polynomial-scaling extension of pCCD to open-shell systems that matches sCI1 in terms of computed energies. In this sense, the present results obtained with ΔsCI1 for open-shell excitations are appealing and encourage the development of a generalized pCCD method.

APPENDIX A: NUMBER OF DETERMINANTS

What is the number of determinants in a given hCI model, defined by the hierarchy h (see eq 1) and the reference determinant? Here we address this question by first working out the simpler case of a closed-shell reference. Then we move to a slightly more complicated case of an open-shell reference with a single unpaired electron. Finally, we deduce the general case. The reference determinant for each case is shown in Figure 5.

The gist of the deduction is as follows. We start from the known number of determinants based only on the excitation degree e. Then we systematically decompose each term into specific contributions based on whether the excitation increases or reduces the seniority. For the decomposition, we make use of Vandermonde's identity:

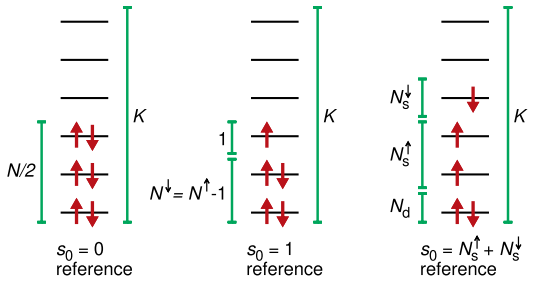

Figure 5. Closed-shell determinant ($s_0 = 0$) with N electrons (left), open-shell determinant ($s_0 = 1$) with $N^{\uparrow}$ spin-up electrons and $N^{\downarrow} = N^{\uparrow} - 1$ spin-down electrons (center), and general determinant ($s_0 = N_s^{\uparrow} + N_s^{\downarrow}$) with N_d doubly occupied orbitals, $N_s^{\uparrow}$ singly occupied spin-up electrons, and $N_s^{\downarrow}$ singly occupied spin-down electrons (right). In the three cases, there are K spatial orbitals. The numbers of determinants generated from these three reference determinants, from left to right, which have excitation degree e and seniority s, are given in eqs A4, A6, and A7.

$$\binom{n}{k} = \sum_{j}^{k} \binom{m}{j}\binom{n-m}{k-j} \tag{A1}$$

Next, an incremental seniority can be assigned to each type of contribution. Finally, the final answer can be obtained by summing only the contributions with the desired seniority s.

We start with the simpler case of a closed-shell determinant with N electrons and K spatial orbitals (left panel of Figure 5). From this reference determinant, the number of excited determinants generated by exciting e electrons is given by[1]

$$\sum_{p=0}^{e} \binom{N/2}{p}\binom{K-N/2}{p}\binom{N/2}{e-p}\binom{K-N/2}{e-p} \tag{A2}$$

where the sum expresses the different combinations for exciting spin-up or spin-down electrons. The first binomial term accounts for the number of possibilities for exciting p spin-up electrons from the $N/2$ orbitals, the second term represents the number of ways of placing these p electrons into $K - N/2$ orbitals, and similarly for the latter two terms and the $e - p$ remaining spin-down electrons.

To account for the seniority of the excited determinants, one must disentangle the excitations based on how they change the seniority number while keeping track of the previously excited electrons. Starting from the closed-shell determinant, p spin-up electrons are excited, which increases the seniority by $2p$ (a factor of p due to the unpaired spin-up electrons just excited, and another factor of p due to the unpaired spin-down electrons left behind). The first two binomial terms in eq A2 are left untouched since they are always accompanied by the same change in seniority. Next, the spin-down electrons can be excited from the same orbitals from which the spin-up electrons were excited (decreasing the seniority by one) or instead from an orbital that remained doubly occupied (increasing the seniority by one). The two possibilities are expressed by decomposing the third binomial term in eq A2 as a sum over the two corresponding binomials, such as

$$\binom{N/2}{e-p} = \sum_{q=0}^{e-p} \binom{p}{q}\binom{N/2-p}{e-p-q} \tag{A3}$$

The first binomial counts the number of possibilities for exciting q spin-down electrons from one of the p orbitals from which a

https://doi.org/10.1021/acs.jctc.3c00946
J. Chem. Theory Comput. 2023, 19, 8654−8670

spin-up electron was already excited. By removing the unpaired spin-down electron left behind, the seniority thus decreases by a factor of q. The second term accounts for the complementary excitations, where the $(e - p - q)$ spin-down electrons are chosen out of the $N/2 - p$ orbitals that remained doubly occupied after exciting the p spin-up electrons. Therefore, this term increases the seniority by $(e - p - q)$. We proceed similarly for the fourth binomial term of eq A2 by decomposing it into the sum of two other binomials, where r spin-down electrons pair with the previously spin-up electrons (thus reducing the seniority) and $(e - p - r)$ do not (which increases the seniority). By collecting the seniority changes from each term, namely, $(2p)$ from the unmodified binomials, $(-q)$ and $(e - p - q)$ from the third binomial, and $(-r)$ and $(e - p - r)$ from the fourth one, the seniority of the excited determinant is given by $s = 2(e - q - r)$. Finally, by combining the seniority-specific binomials and imposing the desired seniority via a Kronecker delta, the number of determinants with a given excitation degree e and seniority s produced from a closed-shell reference $(s_0 = 0)$ is given by

$$\sum_{p=0}^{e} \binom{N/2}{p}\binom{K - N/2}{p} \sum_{q=0}^{e-p} \binom{p}{q}\binom{N/2 - p}{e - p - q} \sum_{r=0}^{e-p} \binom{p}{r}\binom{K - N/2 - p}{e - p - r} \delta_{s,2(e-q-r)} \tag{A4}$$

To obtain the final number of determinants for a given hierarchy h, we simply sum over the allowed combinations of e and s according to eq 1.

Moving to the case where the numbers of spin-up electrons $(N^{\uparrow})$ and spin-down electrons $(N^{\downarrow})$ differ by one $(N^{\uparrow} = N^{\downarrow} + 1)$, which is illustrated in the center panel of Figure 5, the number of excited determinants generated exclusively by exciting e electrons is analogous to eq A2, being given by

$$\sum_{p=0}^{e} \binom{N^{\uparrow}}{p}\binom{K - N^{\uparrow}}{p}\binom{N^{\downarrow}}{e - p}\binom{K - N^{\downarrow}}{e - p} \tag{A5}$$

The deduction proceeds similarly to the closed-shell case. The main differences are the following. The first binomial term of eq A5 is decomposed into the sum of t spin-up electrons excited from the singly occupied orbital and $(p - t)$ that are excited from the $N^{\downarrow}$ doubly occupied ones. The second binomial is left untouched, as before. The third one is also decomposed as explained for the closed-shell case, with the difference that the q spin-down electrons are excited from $(p - t)$ orbitals (instead of p) from which spin-up electrons were excited. Similarly, in the fourth binomial of eq A5, r spin-down electrons are placed into one of the $(1 + p - t)$ orbitals (rather than p in the closed-shell case) which contain an unpaired spin-up electron. Collecting the individual contributions and setting the targeted seniority, the number of determinants generated from an $s_0 = 1$ reference determinant with excitation degree e and seniority s is given by

$$\sum_{p=0}^{e} \sum_{t=0}^{p} \binom{1}{t}\binom{N^{\downarrow}}{p - t}\binom{K - N^{\uparrow}}{p} \sum_{q=0}^{e-p} \binom{p - t}{q}\binom{N^{\downarrow} - p + t}{e - p - q} \sum_{r=0}^{e-p} \binom{1 + p - t}{r}\binom{K - N^{\downarrow} - 1 - p + t}{e - p - r} \delta_{s,1+2(e-q-r-t)} \tag{A6}$$

In the general case, an arbitrary reference determinant is defined by three parameters, the number of doubly occupied orbitals (N_d), the number of singly occupied spin-up electrons $(N_s^{\uparrow} = N^{\uparrow} - N_d)$, and the number of singly occupied spin-down electrons $(N_s^{\downarrow} = N^{\downarrow} - N_d)$. (Alternatively, one could employ the number of electrons N, N_d, and the spin quantum number $S_z = (N^{\uparrow} - N^{\downarrow})/2)$. For K spatial orbitals, the number of virtual orbitals is $N_v = K - N_d - N_s^{\uparrow} - N_s^{\downarrow}$.

The deduction is somewhat more involved but follows along the same lines as the two previously discussed cases. The starting point is also given by eq A5, with each binomial being written as a sum of two or more binomials that distinguish the change in seniority. Here, we just state how each term is decomposed, where the details can be checked by inspection of the final result presented below (see eq A7). The first binomial of eq A5 is decomposed into the contributions of spin-up electrons excited from the N_d doubly occupied orbitals and the $N_s^{\uparrow}$ singly occupied orbitals. The second binomial is decomposed into the spin-up electrons being excited to the N_v virtual orbitals and to the $N_s^{\downarrow}$ singly occupied orbitals. The third one undergoes two decompositions and is thus expressed as a double sum over three binomials. The spin-down electrons are distinguished between the $N_s^{\downarrow}$ singly occupied orbitals, a subset of N_d doubly occupied orbitals for which spin-up electrons were excited, and the complementary subset for which no spin-up electrons were excited. Finally, the fourth binomial of eq A5 counts the number of possibilities to place the excited spin-down electrons. It is first decomposed into two terms, based on whether they are promoted to the N_v virtual orbitals or to the $N_s^{\uparrow}$ singly occupied orbitals. Each term is further decomposed into two terms, accounting for the subset of N_v orbitals which now contain spin-up electrons and the subset of $N_s^{\uparrow}$ orbitals from which spin-up electrons were removed, thus leading to three sums over four binomials. The final result for the number of determinants generated from an arbitrary reference determinant constrained to have excitation degree e and seniority s is given by

$$\sum_{p=0}^{e} \sum_{t=0}^{p} \binom{N_s^{\uparrow}}{t}\binom{N_d}{p - t} \sum_{w=0}^{p} \binom{N_v}{w}\binom{N_s^{\downarrow}}{p - w} \sum_{u=0}^{e-p} \binom{N_s^{\downarrow}}{u} \sum_{v=0}^{e-p-u} \binom{p - t}{v}\binom{N_d - p + t}{e - p - u - v} \sum_{r=0}^{e-p} \sum_{m=0}^{r} \binom{w}{m}\binom{N_v - w}{r - m} \sum_{n=0}^{e-p-r} \binom{t}{n}\binom{N_s^{\uparrow} - t}{e - p - r - n} \delta_{s,N_s^{\uparrow}+N_s^{\downarrow}+2(e+w-p-t-u-v-m-n)} \tag{A7}$$

■ ASSOCIATED CONTENT

Data Availability Statement

The data associated with the PECs and derived properties can be found at https://github.com/kossoski/open_shell_hCI.

Supporting Information

The Supporting Information is available free of charge at https://pubs.acs.org/doi/10.1021/acs.jctc.3c00946.

Definition of the statistical measures; equilibrium geometries of ethylene and vinyl; details about the fitting of potential energy curves; number of determinants of each CI model; potential energy curves for OH, CN, vinyl, and H_7, computed according to FCI and the various hCI, eCI, and sCI models considered here; and convergence of the NPE, distance errors, and equilibrium properties of open-

https://doi.org/10.1021/acs.jctc.3c00946
J. Chem. Theory Comput. 2023, 19, 8654−8670

shell (OH, CN, vinyl, and H_7) and closed-shell (HF, F_2, ethylene, N_2, H_4, and H_8) systems as functions of the number of determinants according to the various CI models considered here while corrected with the standard and the renormalized EN2 perturbative energy (PDF)

For the full set of 50 excited states for closed-shell molecules and 19 excited states for open-shell radicals, total energies and excitation energies obtained with the various hCI, eCI, and sCI models considered here, in both ground-state-based and state-specific approaches; number of determinants in the reference; saddle point order associated with the ΔCSF solutions; reference excitation energies and corresponding methods; and complementary statistical metrics; for a subset of 27 excited states for closed-shell molecules and 15 excited states for radicals, additional total energies and excitation energies obtained with low-order state-specific hCI and eCI models without enforcing spin pure states; for a subset of 16 excited states for closed-shell molecules and six excited states for radicals, additional total energies and excitation energies obtained with higher-order hCI and eCI models (XLSX)

AUTHOR INFORMATION

Corresponding Authors

Fábris Kossoski − *Laboratoire de Chimie et Physique Quantiques (UMR 5626), Université de Toulouse, CNRS, UPS, F-31062 Toulouse, France;* orcid.org/0000-0002-1627-7093; Email: fkossoski@irsamc.ups-tlse.fr

Pierre-François Loos − *Laboratoire de Chimie et Physique Quantiques (UMR 5626), Université de Toulouse, CNRS, UPS, F-31062 Toulouse, France;* orcid.org/0000-0003-0598-7425; Email: loos@irsamc.ups-tlse.fr

Complete contact information is available at: https://pubs.acs.org/10.1021/acs.jctc.3c00946

Notes

The authors declare no competing financial interest.

ACKNOWLEDGMENTS

This work was performed using HPC resources from CALMIP (Toulouse) under allocation 2023-18005. This project received funding from the European Research Council (ERC) under the European Union's Horizon 2020 Research and Innovation Programme (Grant Agreement 863481).

REFERENCES

(1) Szabo, A.; Ostlund, N. S. *Modern Quantum Chemistry*; McGraw-Hill: New York, 1989.

(2) Helgaker, T.; Jørgensen, P.; Olsen, J. *Molecular Electronic-Structure Theory*; John Wiley & Sons, 2013.

(3) Bytautas, L.; Henderson, T. M.; Jiménez-Hoyos, C. A.; Ellis, J. K.; Scuseria, G. E. Seniority and Orbital Symmetry as Tools for Establishing a Full Configuration Interaction Hierarchy. *J. Chem. Phys.* **2011**, *135*, No. 044119.

(4) Allen, T. L.; Shull, H. Electron Pairs in the Beryllium Atom. *J. Phys. Chem.* **1962**, *66*, 2281−2283.

(5) Smith, D. W.; Fogel, S. J. Natural Orbitals and Geminals of the Beryllium Atom. *J. Chem. Phys.* **1965**, *43*, S91−S96.

(6) Veillard, A.; Clementi, E. Complete Multi-Configuration Self-Consistent Field Theory. *Theor. Chim. Acta* **1967**, *7*, 133−143.

(7) Bytautas, L.; Scuseria, G. E.; Ruedenberg, K. Seniority number description of potential energy surfaces: Symmetric dissociation of water, N2, C2, and Be2. *J. Chem. Phys.* **2015**, *143*, No. 094105.

(8) Alcoba, D. R.; Torre, A.; Lain, L.; Oña, O. B.; Capuzzi, P.; Van Raemdonck, M.; Bultinck, P.; Van Neck, D. A hybrid configuration interaction treatment based on seniority number and excitation schemes. *J. Chem. Phys.* **2014**, *141*, No. 244118.

(9) Alcoba, D. R.; Torre, A.; Lain, L.; Massaccesi, G. E.; Oña, O. B. Configuration interaction wave functions: A seniority number approach. *J. Chem. Phys.* **2014**, *140*, No. 234103.

(10) Kossoski, F.; Damour, Y.; Loos, P.-F. Hierarchy Configuration Interaction: Combining Seniority Number and Excitation Degree. *J. Phys. Chem. Lett.* **2022**, *13*, 4342−4349.

(11) Van Raemdonck, M.; Alcoba, D. R.; Poelmans, W.; De Baerdemacker, S.; Torre, A.; Lain, L.; Massaccesi, G. E.; Van Neck, D.; Bultinck, P. Polynomial scaling approximations and dynamic correlation corrections to doubly occupied configuration interaction wave functions. *J. Chem. Phys.* **2015**, *143*, No. 104106.

(12) Alcoba, D. R.; Torre, A.; Lain, L.; Oña, O. B.; Massaccesi, G. E.; Capuzzi, P. Hybrid Treatments Based on Determinant Seniority Numbers and Spatial Excitation Levels in the Configuration Interaction Framework. *Adv. Quantum Chem.* **2018**, *76*, 315−332.

(13) Hurley, A. C.; Lennard-Jones, J. E.; Pople, J. A. The molecular orbital theory of chemical valency XVI. A theory of paired-electrons in polyatomic molecules. *Proc. R. Soc. A* **1953**, *220*, 446−455.

(14) Cullen, J. Generalized valence bond solutions from a constrained coupled cluster method. *Chem. Phys.* **1996**, *202*, 217−229.

(15) Van Voorhis, T.; Head-Gordon, M. The imperfect pairing approximation. *Chem. Phys. Lett.* **2000**, *317*, 575−580.

(16) Parkhill, J. A.; Lawler, K.; Head-Gordon, M. The perfect quadruples model for electron correlation in a valence active space. *J. Chem. Phys.* **2009**, *130*, No. 084101.

(17) Parkhill, J. A.; Head-Gordon, M. A tractable and accurate electronic structure method for static correlations: The perfect hextuples model. *J. Chem. Phys.* **2010**, *133*, No. 024103.

(18) Lehtola, S.; Parkhill, J.; Head-Gordon, M. Cost-effective description of strong correlation: Efficient implementations of the perfect quadruples and perfect hextuples models. *J. Chem. Phys.* **2016**, *145*, No. 134110.

(19) Lehtola, S.; Parkhill, J.; Head-Gordon, M. Orbital optimization in the perfect pairing hierarchy: applications to full-valence calculations on linear polyacenes. *Mol. Phys.* **2018**, *116*, 547−560.

(20) Ziegler, T.; Rauk, A.; Baerends, E. J. On the calculation of multiplet energies by the Hartree-Fock-Slater method. *Theor. Chim. Acta* **1977**, *43*, 261−271.

(21) Burton, H. G. A.; Wales, D. J. Energy Landscapes for Electronic Structure. *J. Chem. Theory Comput.* **2021**, *17*, 151−169.

(22) Shea, J. A. R.; Neuscamman, E. Communication: A mean field platform for excited state quantum chemistry. *J. Chem. Phys.* **2018**, *149*, No. 081101.

(23) Tran, L. N.; Shea, J. A. R.; Neuscamman, E. Tracking Excited States in Wave Function Optimization Using Density Matrices and Variational Principles. *J. Chem. Theory Comput.* **2019**, *15*, 4790−4803.

(24) Tran, L. N.; Neuscamman, E. Improving Excited-State Potential Energy Surfaces via Optimal Orbital Shapes. *J. Phys. Chem. A* **2020**, *124*, 8273−8279.

(25) Hardikar, T. S.; Neuscamman, E. A self-consistent field formulation of excited state mean field theory. *J. Chem. Phys.* **2020**, *153*, No. 164108.

(26) Shea, J. A. R.; Gwin, E.; Neuscamman, E. A Generalized Variational Principle with Applications to Excited State Mean Field Theory. *J. Chem. Theory Comput.* **2020**, *16*, 1526−1540.

(27) Burton, H. G. Energy Landscape of State-Specific Electronic Structure Theory. *J. Chem. Theory Comput.* **2022**, *18*, 1512−1526.

(28) Hanscam, R.; Neuscamman, E. Applying Generalized Variational Principles to Excited-State-Specific Complete Active Space Self-consistent Field Theory. *J. Chem. Theory Comput.* **2022**, *18*, 6608−6621.

(29) Kossoski, F.; Loos, P.-F. State-Specific Configuration Interaction for Excited States. *J. Chem. Theory Comput.* **2023**, *19*, 2258−2269.

(30) Marie, A.; Burton, H. G. A. Excited States, Symmetry Breaking, and Unphysical Solutions in State-Specific CASSCF Theory. *J. Phys. Chem. A* **2023**, *127*, 4538−4552.
(31) Tran, L. N.; Neuscamman, E. Exploring Ligand-to-Metal Charge-Transfer States in the Photo-Ferrioxalate System Using Excited-State Specific Optimization. *J. Phys. Chem. Lett.* **2023**, *14*, 7454−7460.
(32) Filatov, M.; Shaik, S. A spin-restricted ensemble-referenced Kohn-Sham method and its application to diradicaloid situations. *Chem. Phys. Lett.* **1999**, *304*, 429−437.
(33) Kowalczyk, T.; Yost, S. R.; Voorhis, T. V. Assessment of the ΔSCF density functional theory approach for electronic excitations in organic dyes. *J. Chem. Phys.* **2011**, *134*, No. 054128.
(34) Kowalczyk, T.; Tsuchimochi, T.; Chen, P.-T.; Top, L.; Van Voorhis, T. Excitation energies and Stokes shifts from a restricted open-shell Kohn-Sham approach. *J. Chem. Phys.* **2013**, *138*, No. 164101.
(35) Gilbert, A. T.; Besley, N. A.; Gill, P. M. Self-consistent field calculations of excited states using the maximum overlap method (MOM). *J. Phys. Chem. A* **2008**, *112*, 13164−13171.
(36) Barca, G. M.; Gilbert, A. T.; Gill, P. M. Simple Models for Difficult Electronic Excitations. *J. Chem. Theory Comput.* **2018**, *14*, 1501−1509.
(37) Hait, D.; Head-Gordon, M. Excited State Orbital Optimization via Minimizing the Square of the Gradient: General Approach and Application to Singly and Doubly Excited States via Density Functional Theory. *J. Chem. Theory Comput.* **2020**, *16*, 1699−1710.
(38) Hait, D.; Head-Gordon, M. Orbital Optimized Density Functional Theory for Electronic Excited States. *J. Phys. Chem. Lett.* **2021**, *12*, 4517−4529.
(39) Zhao, L.; Neuscamman, E. Density Functional Extension to Excited-State Mean-Field Theory. *J. Chem. Theory Comput.* **2020**, *16*, 164−178.
(40) Levi, G.; Ivanov, A. V.; Jónsson, H. Variational Density Functional Calculations of Excited States via Direct Optimization. *J. Chem. Theory Comput.* **2020**, *16*, 6968−6982.
(41) Carter-Fenk, K.; Herbert, J. M. State-Targeted Energy Projection: A Simple and Robust Approach to Orbital Relaxation of Non-Aufbau Self-Consistent Field Solutions. *J. Chem. Theory Comput.* **2020**, *16*, 5067−5082.
(42) Toffoli, D.; Quarin, M.; Fronzoni, G.; Stener, M. Accurate Vertical Excitation Energies of BODIPY/Aza-BODIPY Derivatives from Excited-State Mean-Field Calculations. *J. Phys. Chem. A* **2022**, *126*, 7137−7146.
(43) Schmerwitz, Y. L. A.; Ivanov, A. V.; Jonsson, E. O.; Jonsson, H.; Levi, G. Variational Density Functional Calculations of Excited States: Conical Intersection and Avoided Crossing in Ethylene Bond Twisting. *J. Phys. Chem. Lett.* **2022**, *13*, 3990−3999.
(44) Schmerwitz, Y. L. A.; Levi, G.; Jónsson, H. Calculations of Excited Electronic States by Converging on Saddle Points Using Generalized Mode Following. *J. Chem. Theory Comput.* **2023**, *19*, 3634−3651.
(45) Clune, R.; Shea, J. A. R.; Neuscamman, E. N5-Scaling Excited-State-Specific Perturbation Theory. *J. Chem. Theory Comput.* **2020**, *16*, 6132−6141.
(46) Zhao, L.; Neuscamman, E. Excited state mean-field theory without automatic differentiation. *J. Chem. Phys.* **2020**, *152*, No. 204112.
(47) Clune, R.; Shea, J. A. R.; Hardikar, T. S.; Tuckman, H.; Neuscamman, E. Studying excited-state-specific perturbation theory on the Thiel set. *J. Chem. Phys.* **2023**, *158*, No. 224113.
(48) Scemama, A.; Garniron, Y.; Caffarel, M.; Loos, P. F. Deterministic Construction Of Nodal Surfaces Within Quantum Monte Carlo: The Case Of FeS. *J. Chem. Theory Comput.* **2018**, *14*, 1395.
(49) Scemama, A.; Benali, A.; Jacquemin, D.; Caffarel, M.; Loos, P. F. Excitation Energies From Diffusion Monte Carlo Using Selected Configuration Interaction Nodes. *J. Chem. Phys.* **2018**, *149*, No. 034108.
(50) Dash, M.; Moroni, S.; Scemama, A.; Filippi, C. Perturbatively Selected Configuration-Interaction Wave Functions for Efficient Geometry Optimization in Quantum Monte Carlo. *J. Chem. Theory Comput.* **2018**, *14*, 4176−4182.
(51) Dash, M.; Feldt, J.; Moroni, S.; Scemama, A.; Filippi, C. Excited States with Selected Configuration Interaction-Quantum Monte Carlo: Chemically Accurate Excitation Energies and Geometries. *J. Chem. Theory Comput.* **2019**, *15*, 4896−4906.
(52) Dash, M.; Moroni, S.; Filippi, C.; Scemama, A. Tailoring CIPSI Expansions for QMC Calculations of Electronic Excitations: The Case Study of Thiophene. *J. Chem. Theory Comput.* **2021**, *17*, 3426−3434.
(53) Cuzzocrea, A.; Moroni, S.; Scemama, A.; Filippi, C. Reference Excitation Energies of Increasingly Large Molecules: A QMC Study of Cyanine Dyes. *J. Chem. Theory Comput.* **2022**, *18*, 1089−1095.
(54) Shepard, S.; Panadés-Barrueta, R. L.; Moroni, S.; Scemama, A.; Filippi, C. Double Excitation Energies from Quantum Monte Carlo Using State-Specific Energy Optimization. *J. Chem. Theory Comput.* **2022**, *18*, 6722−6731.
(55) Otis, L.; Craig, I. M.; Neuscamman, E. A hybrid approach to excited-state-specific variational Monte Carlo and doubly excited states. *J. Chem. Phys.* **2020**, *153*, No. 234105.
(56) Otis, L.; Neuscamman, E. A promising intersection of excited-state-specific methods from quantum chemistry and quantum Monte Carlo. *Wiley Interdiscip. Rev.: Comput. Mol. Sci.* **2023**, *13*, e1659.
(57) Piecuch, P.; Kowalski, K. In Search of the Relationship between Multiple Solutions Characterizing Coupled-Cluster Theories. *Comput. Chem.: Rev. Curr. Trends* **2000**, *5*, 1−104.
(58) Mayhall, N. J.; Raghavachari, K. Multiple Solutions to the Single-Reference CCSD Equations for NiH. *J. Chem. Theory Comput.* **2010**, *6*, 2714−2720.
(59) Lee, J.; Small, D. W.; Head-Gordon, M. Excited States via Coupled Cluster Theory without Equation-of-Motion Methods: Seeking Higher Roots with Application to Doubly Excited States and Double Core Hole States. *J. Chem. Phys.* **2019**, *151*, No. 214103.
(60) Kossoski, F.; Marie, A.; Scemama, A.; Caffarel, M.; Loos, P.-F. Excited States from State-Specific Orbital-Optimized Pair Coupled Cluster. *J. Chem. Theory Comput.* **2021**, *17*, 4756.
(61) Marie, A.; Kossoski, F.; Loos, P.-F. Variational coupled cluster for ground and excited states. *J. Chem. Phys.* **2021**, *155*, No. 104105.
(62) Rishi, V.; Ravi, M.; Perera, A.; Bartlett, R. J. Dark Doubly Excited States with Modified Coupled Cluster Models: A Reliable Compromise between Cost and Accuracy? *J. Phys. Chem. A* **2023**, *127*, 828−834.
(63) Tuckman, H.; Neuscamman, E. Excited-State-Specific Projected Coupled-Cluster Theory. *J. Chem. Theory Comput.* **2023**, *19*, 6160−6171.
(64) Garniron, Y.; et al. Quantum Package 2.0: a open-source determinant-driven suite of programs. *J. Chem. Theory Comput.* **2019**, *15*, 3591.
(65) Limacher, P. A.; Ayers, P. W.; Johnson, P. A.; De Baerdemacker, S.; Van Neck, D.; Bultinck, P. A New Mean-Field Method Suitable for Strongly Correlated Electrons: Computationally Facile Antisymmetric Products of Nonorthogonal Geminals. *J. Chem. Theory Comput.* **2013**, *9*, 1394−1401.
(66) Limacher, P. A.; Kim, T. D.; Ayers, P. W.; Johnson, P. A.; De Baerdemacker, S.; Van Neck, D.; Bultinck, P. The Influence of Orbital Rotation on the Energy of Closed-Shell Wavefunctions. *Mol. Phys.* **2014**, *112*, 853−862.
(67) Tecmer, P.; Boguslawski, K.; Johnson, P. A.; Limacher, P. A.; Chan, M.; Verstraelen, T.; Ayers, P. W. Assessing the Accuracy of New Geminal-Based Approaches. *J. Phys. Chem. A* **2014**, *118*, 9058−9068.
(68) Boguslawski, K.; Tecmer, P.; Ayers, P. W.; Bultinck, P.; De Baerdemacker, S.; Van Neck, D. Efficient Description of Strongly Correlated Electrons with Mean-Field Cost. *Phys. Rev. B* **2014**, *89*, No. 201106.
(69) Boguslawski, K.; Ayers, P. W. Linearized Coupled Cluster Correction on the Antisymmetric Product of 1-Reference Orbital Geminals. *J. Chem. Theory Comput.* **2015**, *11*, 5252−5261.
(70) Boguslawski, K.; Tecmer, P.; Bultinck, P.; De Baerdemacker, S.; Van Neck, D.; Ayers, P. W. Nonvariational Orbital Optimization Techniques for the AP1roG Wave Function. *J. Chem. Theory Comput.* **2014**, *10*, 4873−4882.

https://doi.org/10.1021/acs.jctc.3c00946
J. Chem. Theory Comput. 2023, 19, 8654−8670

(71) Boguslawski, K.; Tecmer, P.; Limacher, P. A.; Johnson, P. A.; Ayers, P. W.; Bultinck, P.; De Baerdemacker, S.; Van Neck, D. Projected Seniority-Two Orbital Optimization of the Antisymmetric Product of One-Reference Orbital Geminal. *J. Chem. Phys.* **2014**, *140*, No. 214114.
(72) Johnson, P. A.; Fecteau, C.-É.; Berthiaume, F.; Cloutier, S.; Carrier, L.; Gratton, M.; Bultinck, P.; De Baerdemacker, S.; Van Neck, D.; Limacher, P.; Ayers, P. W. Richardson-Gaudin mean-field for strong correlation in quantum chemistry. *J. Chem. Phys.* **2020**, *153*, No. 104110.
(73) Henderson, T. M.; Bulik, I. W.; Stein, T.; Scuseria, G. E. Seniority-based coupled cluster theory. *J. Chem. Phys.* **2014**, *141*, No. 244104.
(74) Stein, T.; Henderson, T. M.; Scuseria, G. E. Seniority Zero Pair Coupled Cluster Doubles Theory. *J. Chem. Phys.* **2014**, *140*, No. 214113.
(75) Henderson, T. M.; Bulik, I. W.; Scuseria, G. E. Pair Extended Coupled Cluster Doubles. *J. Chem. Phys.* **2015**, *142*, No. 214116.
(76) Chen, Z.; Zhou, C.; Wu, W. Seniority Number in Valence Bond Theory. *J. Chem. Theory Comput.* **2015**, *11*, 4102−4108.
(77) Bytautas, L.; Dukelsky, J. Seniority based energy renormalization group (Ω-ERG) approach in quantum chemistry: Initial formulation and application to potential energy surfaces. *Comput. Theor. Chem.* **2018**, *1141*, 74−88.
(78) Boguslawski, K. Open-shell extensions to closed-shell pCCD. *Chem. Commun.* **2021**, *57*, 12277−12280.
(79) Tecmer, P.; Boguslawski, K. Geminal-based electronic structure methods in quantum chemistry. Toward a geminal model chemistry. *Phys. Chem. Chem. Phys.* **2022**, *24*, 23026−23048.
(80) Mamache, S.; Gałyńska, M.; Boguslawski, K. Benchmarking ionization potentials using the simple pCCD model. *Phys. Chem. Chem. Phys.* **2023**, *25*, 18023−18029.
(81) Fecteau, C.-É.; Cloutier, S.; Moisset, J.-D.; Boulay, J.; Bultinck, P.; Faribault, A.; Johnson, P. A. Near-exact treatment of seniority-zero ground and excited states with a Richardson−Gaudin mean-field. *J. Chem. Phys.* **2022**, *156*, No. 194103.
(82) Boguslawski, K. Targeting Excited States in All-Trans Polyenes with Electron-Pair States. *J. Chem. Phys.* **2016**, *145*, No. 234105.
(83) Boguslawski, K. Erratum: "Targeting excited states in all-trans polyenes with electron-pair states" [J. Chem. Phys. 145, 234105 (2016)]. *J. Chem. Phys.* **2017**, *147*, No. 139901.
(84) Boguslawski, K. Targeting Doubly Excited States with Equation of Motion Coupled Cluster Theory Restricted to Double Excitations. *J. Chem. Theory Comput.* **2019**, *15*, 18−24.
(85) Nowak, A.; Tecmer, P.; Boguslawski, K. Assessing the accuracy of simplified coupled cluster methods for electronic excited states in f0 actinide compounds. *Phys. Chem. Chem. Phys.* **2019**, *21*, 19039−19053.
(86) Nowak, A.; Boguslawski, K. A configuration interaction correction on top of pair coupled cluster doubles. *Phys. Chem. Chem. Phys.* **2023**, *25*, 7289−7301.
(87) Krylov, A. I. Spin-Flip Equation-of-Motion Coupled-Cluster Electronic Structure Method for a Description of Excited States, Bond Breaking, Diradicals, and Triradicals. *Acc. Chem. Res.* **2006**, *39*, 83−91.
(88) Horbatenko, Y.; Sadiq, S.; Lee, S.; Filatov, M.; Choi, C. H. Mixed-Reference Spin-Flip Time-Dependent Density Functional Theory (MRSF-TDDFT) as a Simple yet Accurate Method for Diradicals and Diradicaloids. *J. Chem. Theory Comput.* **2021**, *17*, 848−859.
(89) Monino, E.; Boggio-Pasqua, M.; Scemama, A.; Jacquemin, D.; Loos, P.-F. Reference Energies for Cyclobutadiene: Automerization and Excited States. *J. Phys. Chem. A* **2022**, *126*, 4664−4679.
(90) Chilkuri, V. G.; Applencourt, T.; Gasperich, K.; Loos, P.-F.; Scemama, A. Spin-Adapted Selected Configuration Interaction in a Determinant Basis. *Adv. Quantum Chem.* **2021**, *83*, 65.
(91) Maurice, D.; Head-Gordon, M. On the Nature of Electronic Transitions in Radicals: An Extended Single Excitation Configuration Interaction Method. *J. Phys. Chem.* **1996**, *100*, 6131−6137.
(92) Huron, B.; Malrieu, J. P.; Rancurel, P. Iterative perturbation calculations of ground and excited state energies from multiconfigurational zeroth-order wavefunctions. *J. Chem. Phys.* **1973**, *58*, 5745−5759.
(93) Giner, E.; Scemama, A.; Caffarel, M. Using perturbatively selected configuration interaction in quantum Monte Carlo calculations. *Can. J. Chem.* **2013**, *91*, 879−885.
(94) Giner, E.; Scemama, A.; Caffarel, M. Fixed-node diffusion Monte Carlo potential energy curve of the fluorine molecule F2 using selected configuration interaction trial wavefunctions. *J. Chem. Phys.* **2015**, *142*, No. 044115.
(95) Garniron, Y.; Scemama, A.; Giner, E.; Caffarel, M.; Loos, P. F. Selected Configuration Interaction Dressed by Perturbation. *J. Chem. Phys.* **2018**, *149*, No. 064103.
(96) Garniron, Y.; Scemama, A.; Loos, P.-F.; Caffarel, M. Hybrid Stochastic-Deterministic Calculation of the Second-Order Perturbative Contribution of Multireference Perturbation Theory. *J. Chem. Phys.* **2017**, *147*, No. 034101.
(97) Davidson, E. R. The iterative calculation of a few of the lowest eigenvalues and corresponding eigenvectors of large real-symmetric matrices. *J. Comput. Phys.* **1975**, *17*, 87−94.
(98) Loos, P.-F.; Scemama, A.; Boggio-Pasqua, M.; Jacquemin, D. Mountaineering Strategy to Excited States: Highly Accurate Energies and Benchmarks for Exotic Molecules and Radicals. *J. Chem. Theory Comput.* **2020**, *16*, 3720−3736.
(99) Véril, M.; Scemama, A.; Caffarel, M.; Lipparini, F.; Boggio-Pasqua, M.; Jacquemin, D.; Loos, P.-F. QUESTDB: a database of highly-accurate excitation energies for the electronic structure community. *Wiley Interdiscip. Rev.: Comput. Mol. Sci.* **2021**, *11*, No. e1517.
(100) Bally, T.; Masamune, S. Cyclobutadiene. *Tetrahedron* **1980**, *36*, 343−370.
(101) Tallarico, J. A.; Randall, M. L.; Snapper, M. L. Intramolecular Cycloadditions between Cyclobutadiene and Alkenes. *J. Am. Chem. Soc.* **1996**, *118*, 9196−9197.
(102) Stanton, J. F.; Gauss, J. Analytic energy derivatives for ionized states described by the equation-of-motion coupled cluster method. *J. Chem. Phys.* **1994**, *101*, 8938−8944.
(103) Kamiya, M.; Hirata, S. Higher-order equation-of-motion coupled-cluster methods for ionization processes. *J. Chem. Phys.* **2006**, *125*, No. 074111.
(104) Bomble, Y. J.; Saeh, J. C.; Stanton, J. F.; Szalay, P. G.; Kállay, M.; Gauss, J. Equation-of-motion coupled-cluster methods for ionized states with an approximate treatment of triple excitations. *J. Chem. Phys.* **2005**, *122*, No. 154107.
(105) Rowe, D. J. Equations-of-Motion Method and the Extended Shell Model. *Rev. Mod. Phys.* **1968**, *40*, 153−166.
(106) Monkhorst, H. J. Calculation of properties with the coupled-cluster method. *Int. J. Quantum Chem.* **1977**, *12*, 421−432.
(107) Koch, H.; Jensen, H. J. A.; Jørgensen, P.; Helgaker, T. Excitation Energies from the Coupled Cluster Singles and Doubles Linear Response Function (CCSDLR). Applications to Be, CH^+, CO, and H_2O. *J. Chem. Phys.* **1990**, *93*, 3345−3350.
(108) Stanton, J. F.; Bartlett, R. J. The equation of motion coupled-cluster method. A systematic biorthogonal approach to molecular excitation energies, transition probabilities, and excited state properties. *J. Chem. Phys.* **1993**, *98*, 7029−7039.
(109) Loos, P. F.; Scemama, A.; Blondel, A.; Garniron, Y.; Caffarel, M.; Jacquemin, D. A Mountaineering Strategy to Excited States: Highly Accurate Reference Energies and Benchmarks. *J. Chem. Theory Comput.* **2018**, *14*, 4360.
(110) Loos, P. F.; Lipparini, F.; Boggio-Pasqua, M.; Scemama, A.; Jacquemin, D. A Mountaineering Strategy to Excited States: Highly-Accurate Energies and Benchmarks for Medium Sized Molecules. *J. Chem. Theory Comput.* **2020**, *16*, 1711−1741.

https://doi.org/10.1021/acs.jctc.3c00946
J. Chem. Theory Comput. 2023, 19, 8654−8670